(NASA-CR-177183). ACTIVE CONTROL OF TORQUE PARTICIPATION CORRELATION Semiannual Progress Report (Catholic Univ. of America) 54 p
CSCL 13I

N87-11994

Unclas
G3/37 44912

SCHOOL OF ENGINEERING & ARCHITECTURE

The Catholic University of America

Washington, DC 20064

NAG 5-780

SEMI-ANNUAL PROGRESS REPORT

ON

ACTIVE CONTROL OF ROBOT MANIPULATOR COMPLIANCE

By

Charles C. Nguyen, Principal Investigator

Farhad J. Pooran,Graduate Research Assistant

Department of Electrical Engineering

The Catholic University of America

Washington D.C. 20064

Submitted to

NASA
GODDARD SPACE FLIGHT CENTER

Greenbelt,Maryland

Attention Mr. Timothy Premack Code 731.4

November 1986

SUMMARY

This progress report summarizes the research work performed at The Catholic University Of America on the research grant entitled "Active Control of Robot Manipulator Compliance, " (Grant#: NAG 5-780) , supported by NASA/Goddard space Flight Center during the period of May 15th, 1986 to November 15th, 1986.

In this report we first present the modelling of the two-degree-of-freedom robot. Then the complete system including the robot and the hybrid controller is simulated on an IBM-XT Personal Computer. Simulation results showed that proper adjustments of controller gains enable the robot to perform successful operations. Further research should focus on developing a guideline for the controller gain design to achieve system stability.

CONTENTS

TABLE OF SYMBOLS

Values are given in SI Units.

A_i	vector from origin of compliant platform to lower attachment points of actuator i with respect to the fixed coordinate system
$A_{i,m}$	known vector in moving coordinate system from origin of moving coordinate system to lower attachment point of actuator i
B_i	known vector in fixed coordinate system from origin of fixed coordinate system to upper attachment point of actuator i
d	known distance between the upper attachment points of actuators 1 and 2
F	force
f( )	vector function
F_e	vector of force error in Cartesian variables

F_d	vector of desired force
f_m	actuating forces
f_y	reaction force
g	acceleration of gravity
I	inertia moment
[I]	Identity matrix
J	Jacobian
K_E	stiffness of the reaction surface
K_{rp}, K_{rf}	proportional controller gains for position and force, respectively
K_{rpd}	derivative controller gain
l_i	vector in fixed coordinate system from upper attachment point to lower attachment point of actuator i
$\|l_i\|_a$	actual magnitude of actuator i obtained by measurement

L	Lagrangian
m, M	mass
P	potential energy
q_i	generalized coordinates
Q_i	generalized forces
q_e	vector of position error in joint variables
R	vector in fixed coordinate system from origin of fixed coordinate system to origin of moving coordinate system
r_i	vector in fixed coordinate system from origin of fixed coordinate system to lower attachment point of actuator i
S	compliance selection vector
T	kinetic energy
$[T]$	Euler angle transformation matrix

T_θ	torque
u_{rp}	error in length due to the error in position
u_{rf}	error in length due to the error in force
V	velocity
X_d	vector of desired Cartesian position
X_e	vector of position error in Cartesian variables
$\dot{X}_e$	vector of velocity error in Cartesian variables
y_E	position of the reaction surface
α	unknown parameter vector which is vector of root of f( )
w	angular velocity
$\dot{w}$	angular acceleration
ψ, θ, Φ	angular orientation of moving platform
Λ	position compensation function

1. INTRODUCTION

Robotics has many potential space applications that can be found in the space station research program [1], such as autonomous repair and replacement capability, automated maintenance, etc. One of the most essential robotic tasks is the assembly of large strucutures in space. Product assembly in space such as mating and fastening of parts requires a very high precision. There is however a tolerance problem that exists in assembly. The positional tolerance of many assembly tasks are quite high (thousands of inch), while those of a robot manipulators are only of the orders of inch. To solve this problem, compliance can be provided to the manipulator so that it can comply with the task-imposed constraint [2]. Compliant motion control is concerned with the control of a robot in contact with its environment [3]. Compliance can be provided passively by the deformation of a mechanical structure, such as mechanical spring or actively by a control system employing force sensors [4-5].

In many applications, there is a need for simultaneous control of positon and force. There are two approaches to compliant motion control. Impedance or stiffness control

specifies dynamic relationships between force and position but do not specify desired forces or positions [3]. Hybrid control that controls position/orientation along specified degrees of freedom and independently controls force/torque along the remaining degrees of freedom [6]. The hybrid control is more suitable for planning a manipulator task and in this report we will present the development of a hybrid controller [7] for a six-degree-of-freedom robot recently built at NASA/GSFC [8] to study robotic assembly in space.

Since the dynamic equations of a six-degree-of-freedom robot is highly complicated, we start our design with a two-degree-of-freedom model. The results of simulated system will be presented and discussed.

2. THE NASA ROBOT

Recently a six-degree-of-freedom robot was built at the GODDARD SPACE FLIGHT CENTER (GSFC) to study the automated assembly of NASA hardware [8] for potential applications in the space station [1]. The robot consists mainly of a lower fixed platform, an upper movable platform and an intelligent end effector (IEE) (Fig. 1A). The movable platform is supported above the fixed platform by six axial rods that are extensible by recirculating ball screws. Six stepper motors were used to derive the ball screws and consequently the movable platform to provide

the gross motion of the IEE. The IEE is attached to another platform suspended from the movable platform by six spring-loaded pistons that provide passive compliance to the IEE by permitting strain on two opposing springs acting in the piston (Fig. 1B). Using force feedback, the robot has been able to perform several assembly tasks such as inserting a peg into the hole, screwing a bolt into a threaded hole. However, since the compliance was provided passively, the assembly process was very slow, for example, the robot took 3 minutes to complete the inserting of a peg into a hole. Therefore, research effort has been made to study the implementation of the hybrid control scheme into the robot system so that the IEE compliance can be provided actively by six electromechanical actuators replacing the existing spring-loaded pistons [10].

3. THE HYBRID CONTROL SCHEME

In many applications, it is necessary to control simultaneously position and force. Such control is called hybrid control, that controls position /orientation along specified degrees of freedom and independently controls force/torque along the remaining degrees of freedom. The degrees of freedom are in a Cartesian coordinate system which is called the constraint frame and is denoted by the symbol [C] [11-13]. In a hybrid controller scheme, each actuator control signal is composed of several components, one for each force

controlled degree of freedom in [C] and one for each position controlled degree of freedom. The actuator signal is computed by [7]:

$$T_i = \sum_{j=1}^{N} \{ \Gamma_{ij} [s_j \ \Delta f_j] + \psi_{ij} [(1-s_j) \ \Delta X_j] \} \qquad (1)$$

Where

T_i=torque applied by the ith actuator

Δf_j=force error in jth degree of freedom of [C].

ΔX_j=position error in jth degree of freedom of [C].

Γ_{ij} and ψ_{ij} = force and position compensation functions, respectively, for the jth input and the jth output.

S_j=component of comliance selection vector.

The compliance selection vector S, is a binary N-tuple that specifies which degrees in [C] are under force control (sjj=1) and which are under position control (sjj=0).

Fig. 2 illustrates the implementation of the hybrid control scheme into existing NASA robot. The complete robot system consists of a position sensor, a six-degree-of-freedom force sensor, 12 controllers with 6 controllers for the position control loop and 6 controllers for the force/torque control loop, 6 linear actuators and the NASA robot. The compliance selection matrix is a (6x6) diagonal matrix.

Two feedback loops compute errors in both applied force/torque and actual position, with the lower loop

controlling the force/torqe. The two independent feedback loops with 6 controllers, provide the drive signals to the actuators[10].

Current research does not prescribe particular control laws for the regulation of errors [7]. Therefore, our research objective is to make a comparative evaluation of different types of control laws in order to select an optional set of controllers for a particular robotic assembly task. Doing this a guideline can be developed for the design of these controllers. The controllers and the coordinate transformations are then implemented on an appropriate computer.

4. COORDINATE TRANSFORMATIONS

There are two coordinate transformations , one for transforming coordinate from Cartesian space into joint space, and one from joint to Cartesian space. With the arrangement of the linear actuators as seen on Fig. 1, the robot does not have independent drive systems for each degree of freedom. The precision motion is achieved in all degrees of freedom by a combination of actuator extension. Therefore, a transformation transforming desired position and orientation of the IEE into actuator extensions is needed. This problem is well-known as an inverse kinematic problem [15] that in general , has non-unique solutions and is very difficult to solve because of non-linearity. However, since the NASA robot has a

special configuration, its inverse kinematic problem has a unique closed-form solution.

On the other hand, the forward kinematic problem of the NASA robot does not have a closed-form solution and is solved iteratively. As part of the hardware, six linear voltage differential transformers (LVDT) are mounted parallel to the six linear actuators to measure their extensions. Position feedback is then achieved by taking the actual extension available from measurements and transforming them into the position and orientation of the IEE. This problem is a forward kinematic problem of an open loop robot like the Stanford manipulator.

Fig. 3 shows the general orientation of the manipulator with two coordinate systems, and Fig. 4 illustrates the vector relationships between the origins of each coordinate system and the actuator attachment point of each platform. These relationships yield the vector equations

$$\mathbf{r}_i = \mathbf{A}_i + \mathbf{R} \qquad (2a)$$

$$\mathbf{r}_i = \mathbf{B}_i + \mathbf{l}_i \qquad (2b)$$

Subtracting (2b) from (2a) and solving for $\mathbf{l}_i$ yields

$$\mathbf{l}_i = \mathbf{A}_i + \mathbf{R} - \mathbf{B}_i \qquad (3)$$

where $\mathbf{l}_i$ is defined with respect to the fixed reference frame.

Since the known vectors $\mathbf{A}_{i,m}$ are defined with respect to

the moving frame, we must apply an Euler angle transformation in order to get the corresponding vector A_i in the fixed reference frame. Applying this transformation, we obtain

$$l_i=[T]^T A_{i,m}+R-B_i \qquad (4)$$

In Equation (4) $A_{i,m}$ and B_i are known constant vectors and R and $[T]^T$ are calculated from the given values of x,y,z, ψ, θ and Φ.

The inverse could be obtained if the vectors l_i were available, but LVDT measures only the magnitude of the corresponding actuator length $|l_i|_a$ and not the required vector. However, because of its closed-loop configuration, the forward kinematics problem of the NASA robot can be solved by solving six nonlinear equations with six unknowns (x,y,z, ψ, θ and Φ). Newton-Raphson method is employed to solve this problem [16].

The iteration formula has the form

$$\alpha_{n+1}=\alpha_n-\left[\frac{\partial f(\alpha_n)}{\partial \alpha_n}\right]^{-1} f(\alpha_n) \qquad (5)$$

Knowing the actual magnitude of the actuators, function $f_i(\alpha)$ can be defined as

$$f_i(\alpha)=l_i^T l_i-|l_i|_a^2 \qquad (6a)$$

where

$$\alpha = \begin{bmatrix} x \\ y \\ z \\ \psi \\ \theta \\ \Phi \end{bmatrix} \tag{6b}$$

and

$$f(\alpha) = \begin{bmatrix} f_1(\alpha) \\ f_2(\alpha) \\ .... \\ .... \\ .... \\ f_6(\alpha) \end{bmatrix} \tag{6c}$$

and $|l_i|_a$ is the actual magnitude of the actuator i obtained from measurement. Using an appropriate set of initial conditions, Equation (5) is repeated until desired accuracy is met.

The Newton-Raphson's method has been applied in the NASA passive compliant robot system to update the position of the compliant platform relative to the compliant base and to compute the position of the movable platform with respect to the fixed platform [8]. This technique requires ample memory and enormous computation time. Therefore, it is suggested to investigate other Newton-Raphson's method. Some of these methods are known as Quasi-Newton methods [17-18]. The Newton-Raphson's iteration diverges if the initial guess is not close to a correct solution [19]. Using Newton-Raphson-Kantorovich theorem [18] it is possible to find how close the initial

guess should be.Consequently, to assure the convergence of the Newton-Raphson iteration it is necessary to implement the Newton-Raphson-Kantorovich theorem using computer software [10].

5. The 2-DEGREE-OF-FREEDOM ROBOT

In order to examine the performance of proposed hybrid control scheme, we begin our study with the 2-degree-of-freedom robot since the dynamic behaviour of the complete six-degree-of-freedom robot is highly complex.

Fig. 5 illustrates a simplified version of the physical robot consisting of 2 linear actuators, 2 LVDT's, 2 force sensors and an IEE. The actuators are connected to a fixed platform using one-degree-of-freedom gimbals. The LVDT's are mounted parallel to the actuators to measure the lengths l_1 and l_2. The 2 force sensors are mounted in series with actuators to measure the reaction forces in the direction of the actuator axes.

5.1 KINEMATICS OF THE MANIPULATOR

Manipulator kinematics is a study of the geometry of manipulator arm without regard to the forces which cause it. In this section, the mathematical relations required to describe the system motion and the fundamental equations that govern kinematic behavior are derived.

5.1.1 POSITON ANALYSIS

The position of the point P at the tip of the hand with respect to the X-Y coordinate (Cartesian frame) is known if its horizontal and vertical projections x, and y are known [10]. However, only the lengths l_1 and l_2 are known from the LVDT's. From the geometry of Fig. 6, we obtain

$$x^2 + y^2 = l_1^2 \tag{7}$$

and $$(d-x)^2 + y^2 = l_2^2 \tag{8}$$

where d is known from the geometry of the system. Since l_1 and l_2 are variables from measurements, we can rewrite Equations (7) and (8) as

$$f_1(x,y) = x^2 + y^2 - l_1^2 = 0 \tag{9}$$

$$f_2(x,y) = (d-x)^2 + y^2 - l_2^2 = 0 \tag{10}$$

To solve these equations for x and y, we can use iteration techniques such as Newton-Raphson method which was described in section 4. For 2-degree-of-freedom case, the equations can be solved by analitical method. Simplifying Equation (8) as

$$x^2 + y^2 + d^2 - 2dx = l_2^2 \tag{11}$$

and substituting $(x^2 + y^2)$ from Equations (7) into (11), we obtain

$$l_1^2 + d^2 - 2dx = l_2^2 \qquad (12)$$

Solving for x yields

$$x = \frac{l_1^2 - l_2^2 + d^2}{2d} \qquad (13)$$

Substituting the value of x into Equation (7)

$$\left[\frac{l_1^2 - l_2^2 + d^2}{2d}\right]^2 + y^2 = l_1^2 \qquad (14)$$

and solving for y we get

$$y = \frac{[4d^2 l_1^2 - (l_1^2 - l_2^2 + d^2)^2]^{1/2}}{2d} \qquad (15)$$

5.1.2 VELOCITY DERIVATION

A manipulator can, in general, be described as a series of links connected at joints. The angles between the links, called the joint angles, are typical joint variables. However, some type of links (prismatic joints) can grow longer, and in that case the joint variable may actually be the length of the link [6].

The position of all the links of a manipulator of n degrees of freedom can be specified with a set of n joint variables. This set of variables is often referred to as

the nx1 joint vector. The space of all such joint vectors is referred to as joint space. There are three representations of a manipulator's position and orientation: descriptions in actuator space, joint space and Cartesian space[15].

In section 5.1.1, we derived the kinematic equations of the hand in Cartesian coordinate system. The forward kinematic transform for this manipulator relates the X-Y position of the hand to the joint variables. For our 2-degree-of-freedom robot with two prismatic actuators, the joint variables can be chosen any of the following sets: (l_1, θ_1), (l_2, θ_2), (θ_1, θ_2) and (l_1, l_2). As the LVDT's can measure the lengths (l_1, l_2), we chose these variables as the joint variables. The inverse kinematic relates the set of joint variables to the desired position and orientation of the hand relative to Cartesian coordinates (Equations (7) and (8)).

In order to move the end-effector in a specified direction at a specified speed, it is necessary to coordinate the motion of the individual joints. For this purpose we drive the differential relationships between the joint displacement and the hand location [3]. The velocity relationship between the joints and hand is determined by the manipulator Jacobian

$$V = J\dot{l}. \qquad (16a)$$

Differentiating Equations (13) and (15) with respect to time

$$\dot{x} = \frac{2l_1\dot{l}_1 - 2l_2\dot{l}_2}{2d} \qquad (16b)$$

or

$$\dot{x} = \frac{1}{d}(l_1\dot{l}_1 - l_2\dot{l}_2) \qquad (17)$$

and

$$\dot{y} = \frac{1}{2d}\left\{\frac{1}{2}[8d^2 l_1\dot{l}_1 - 2(2l_1\dot{l}_1 - 2l_2\dot{l}_2)(l_1^2 - l_2^2 + d^2)][4d^2 l_1^2 - (l_1^2 - l_2^2 + d^2)^2]^{-\frac{1}{2}}\right\} \qquad (18)$$

or

$$\dot{y} = \frac{1}{4d}\{8d^2 l_1\dot{l}_1 - 4l_1(l_1^2 - l_2^2 + d^2)\dot{l}_1 + 4l_2(l_1^2 - l_2^2 + d^2)\dot{l}_2\}$$

$$[4d^2 l_1^2 - (l_1^2 - l_2^2 + d^2)^2]^{-\frac{1}{2}}$$

$$= \frac{1}{4d}[(8d^2 l_1 - 4l_1^3 + 4l_1 l_2^2 - 4l_1 d^2)\dot{l}_1 + 4l_2(l_1^2 - l_2^2 + d^2)\dot{l}_2]$$

$$[4d^2 l_1^2 - (l_1^2 - l_2^2 + d^2)^2]^{-\frac{1}{2}} \qquad (19)$$

Rewriting the Equations (17) and (19) yield

$$\dot{x} = (l_1/d)\dot{l}_1 - (l_2/d)\dot{l}_2 \qquad (20)$$

and

$$\dot{y} = \frac{l_1(d^2 + l_2^2 - l_1^2)}{d\Omega}\dot{l}_1 + \frac{l_2(d^2 + l_1^2 - l_2^2)}{d\Omega}\dot{l}_2 \qquad (21)$$

where

$$\Omega = [4d^2 l_1^2 - (l_1^2 - l_2^2 + d^2)^2]^{\frac{1}{2}} \qquad (22)$$

Writing in vector form

$$\begin{bmatrix}\dot{x}\\ \dot{y}\end{bmatrix}=\begin{bmatrix}A_1 & A_2\\ A_3 & A_4\end{bmatrix}\begin{bmatrix}\dot{l}_1\\ \dot{l}_2\end{bmatrix} \qquad (23)$$

Thus the matrix

$$J=\begin{bmatrix}A_1 & A_2\\ A_3 & A_4\end{bmatrix} \qquad (24)$$

is the manipulator Jacobian,

Where

$$A_1=l_1/d \quad , \quad A_2=-l_2/d \quad , A_3=[l_1(d^2+l_2^2-l_1^2)]/d0$$

and $$A_4=[l_2(d^2+l_1^2-l_2^2)]/d0 \quad .$$

Note that the elements of the Jacobian are functions of joint displacements, and therefore vary with the arm configuration.

5.1.3 ACCELERATION DERIVATION

The linear acceleration of point P with respect to Cartesian system can be obtained by differentiating Equations (20) and (21) as the following:

$$\ddot{x}=(l_1/d)\ddot{l}_1-(l_2/d)\ddot{l}_2+\dot{l}_1^2/d-\dot{l}_{2/d}^2 \qquad (25)$$

or

$$\ddot{x}=[l_1\ddot{l}_1-l_2\ddot{l}_2+\dot{l}_1^2-\dot{l}_2^2]/d \qquad (26)$$

$$\ddot{y}=\frac{(B_1\dot{l}_1^2+2l_1l_2\dot{l}_1\dot{l}_2-2l_1\dot{l}_1^2)}{d\theta}-\frac{4B_1d\,l_1\dot{l}_1^2-2B_1B_2(l_1\dot{l}_1^2-l_1\dot{l}_1\dot{l}_2\dot{l}_2)}{d\theta^3}$$

$$+\left(\frac{l_1B_1}{d\theta}\right)\ddot{l}_1+\frac{(B_2\dot{l}_2^2+2l_1l_2\dot{l}_1\dot{l}_2-2l_2\dot{l}_2^2)}{d\theta}+\left(\frac{l_2B_2}{d\theta}\right)\ddot{l}_2$$

$$-\frac{4d^2B_2l_1\dot{l}_1l_2\dot{l}_2-2B_2(l_1\dot{l}_1l_2\dot{l}_2-l_2^2\dot{l}_2^2)}{d\theta^3} \qquad (27)$$

where

$$B_1=d^2+l_2^2-l_1^2 \quad \text{and} \quad B_2=d^2+l_1^2-l_2^2 \qquad (28)$$

5.2 DYNAMICS OF THE MANIPULATOR

The dynamic behavior can be described in terms of the rate of change of the arm configuration in relation to the joint torques exerted by the actuator [3]. Equations of motions, govern the dynamic reponse of the arm linkage to input joint torque. There are two methods to obtain the

equations of motion: Newton-Euler, and Lagrangian formulation.

5.2.1 NEWTON-EULER FORMULATION

The equation of motion is derived by the direct dynamic system interpretation of Newton's Second Law of Motions, which describes dynamic system in terms of force and momentum. The equations include the constraint forces acting between adjacent links which must be eliminated. The dynamic equations of a rigid body can also be represented by two equations:

i)Newton's equation of motion for a mass particle, which is the translational motion of the center of mass (centroid). For a rigid body where center of mass is accelerating with $\dot{V}_C$, the force F, acting at the center of mass is

$$F_i = m_i \dot{V}_{Ci} \qquad (29)$$

where, m is the total mass of the body, V_{Ci} , the linear velocity of the centroid of link i with respect to the base coordinates (inertial reference frame), and $m_i \dot{V}_{Ci}$, inertial force [15].

ii)Euler's equation of motion, which is the rotational

motion of the centroid. For a rigid body rotating with angular velocity w, and angular acceleration $\dot{w}$, the moment N, which must be acting on the body to cause this motion is

$$N=I_c\dot{w}+w\times I_c w \qquad (30)$$

where I_c is the inertia moment of the body, $I_c\dot{w}$ inertia torque, and $I_c w$ is the angular momentum.

5.2.2 LAGRANGIAN FORMULATION

In the Lagrangian method, the system dynamic behavior is described in terms of work and energy, using generalized coordinates. All the workless forces and constraint forces are automatically eliminated in this method. The resultant equations are generally compact and provide a closed-form expression in terms of joint torques and joint displacements. Furthermore, the derivation is simpler and more systematic than in the Newton-Euler approach. As in kinematics, we need to solve the inverse problem of finding the necessary input torques to obtain a desired output motion (inverse dynamics).

Let q_1 , ..., q_n be generalized coordinates, T and P the total kinetic and potential energy stored in the dynamic system. We define the Lagrangian "L" by

$$L(q_i,\dot{q}_i)=T-P \qquad (31)$$

or

$$d/dt(\partial L/\partial \dot{q}_i)-\partial L/\partial q_i=Q_i \qquad i=1,....n \qquad (32)$$

where Q_i is the generalized forces corresponding to the generalized coordinates q_i.

5.2.3 EQUATIONS_OF_MOTION

To formulate the equations of motion of the robot, we employ the Lagrangian and Newton-Euler approaches.

i) Lagrangian method

Fig. 6 represents the forces acting on the robot system. The robot task is to keep in contact with a reaction surface while maintaining a constant applied force f_0 . This task occurs for example in the process of painting a surface. The robot is moving in a horizontal plane (to the right), while maintaining a constant vertical force on the reaction table. For simplicity, we assume that the table is smooth enough so that the table friction is negligible, joint and actuator friction are also negligible. Therefore, the reaction force will be normal to the hand (f_y).

Using the Lagrangian formulation, we will derive the equations in terms of the two independent joint variables,

the length l_1 and the angle θ_1 [21].

We begin by computing the velocity of the centroids C_1 , C_2 and the end-effetor P. From geometry, the Cartesian positions are

$$x_P = l_1 \cos\theta_1 \tag{33}$$

$$y_P = -l_1 \sin\theta_1 \tag{34}$$

$$x_{C1} = (l_1/2)\cos\theta_1 \tag{35a}$$

and $$y_{C1} = -(l_1/2)\sin\theta_1 \tag{35b}$$

Similarly,

$$x_{C2} = d-(l_2/2)\cos\theta_2 \tag{36a}$$

and $$y_{C2} = -(l_2/2)\sin\theta_2 \tag{36b}$$

To eliminate θ_2 and l_2 from the equations, we can write

$$l_1\cos\theta_1 = d - l_2\cos\theta_2 \tag{37}$$

and $$-l_1\sin\theta_1 = -l_2\sin\theta_2 \tag{38}$$

Substituting from Eqs. (37) and (38) into (36a) and (36b) we get

$$x_{C2} = d-(d-l_1\cos\theta_1)/2 = (d+l_1\cos\theta_1)/2 \tag{39}$$

and $$y_{C2} = -l_1\sin\theta_1/2 \tag{40}$$

Differentiating the above equations with respect to time yields the Cartesian velocities as

$$V_P = \begin{bmatrix} \dot{x} \\ \dot{y} \end{bmatrix} = \begin{bmatrix} \dot{l}_1 \cos\theta_1 - l_1 \sin\theta_1 \dot{\theta}_1 \\ -\dot{l}_1 \sin\theta_1 - l_1 \cos\theta_1 \dot{\theta}_1 \end{bmatrix} = \begin{bmatrix} \cos\theta_1 & -l_1 \sin\theta_1 \\ \sin\theta_1 & -l_1 \cos\theta_1 \end{bmatrix} \begin{bmatrix} \dot{l}_1 \\ \dot{\theta}_1 \end{bmatrix} \qquad (41)$$

and

$$V_{C1} = V_{C2} = \begin{bmatrix} (\dot{l}_1 \cos\theta_1 - l_1 \sin\theta_1 \dot{\theta}_1)/2 \\ -(\dot{l}_1 \sin\theta_1 + l_1 \cos\theta_1 \dot{\theta}_1)/2 \end{bmatrix} \qquad (42)$$

The magnitude of the velocity vectors can now be computed as

$$V_{C1}^2 = V_{C2}^2 = (\dot{x}_1)^2 + (\dot{y}_1)^2 \qquad (43a)$$

or

$$V_{C1}^2 = V_{C2}^2 = 1/4[(\dot{l}_1 \cos\theta_1)^2 + (l_1 \sin\theta_1 \dot{\theta}_1)^2 - 2l_1 \dot{l}_1 \sin\theta_1 \cos\theta_1 \dot{\theta}_1] +$$
$$1/4[(\dot{l}_1 \sin\theta_1)^2 + (l_1 \cos\theta_1 \dot{\theta}_1)^2 + 2l_1 \dot{l}_1 \sin\theta_1 \cos\theta_1 \dot{\theta}_1] \qquad (43b)$$

or $$V_{C1}^2 = V_{C2}^2 = (\dot{l}_1^2 + l_1^2 \dot{\theta}_1^2)/4 \ . \qquad (43c)$$

Similarly,

$$V_P^2 = \dot{l}_1^2 + l_1^2 \dot{\theta}_1^2 \qquad (44)$$

The kinetic energy of a mass m with linear velocity V and angular velocity w is

$$T = 1/2\ mV^2 + 1/2\ Iw^2 \qquad (45a)$$

Note that as we assumed point mass, then the moment of inertia $I_1 = I_2 = 0$, thus $Iw^2 = 0$.

Therefore,

$$T=\Sigma(1/2\ m_i V_i^2) \qquad i=1,\ldots,N \qquad (46a)$$

$$T=1/2\ M_1 V_{C1}^2 +1/2\ M_2 V_{C2}^2 +1/2 M_3 V_P^2 \qquad (46b)$$

where M_1, M_2 and M_3 are the masses of the two linear actuators and the IEE, respectively. Substituting the values of the velocities into (46b) yields

$$T=[(M_1+M_2)/8+M_3/2](\dot{l}_1^2 +l_1^2\dot{\theta}_1^2) \qquad (46c)$$

The actuators are assumed to have identical masses, $M_1=M_2=M$. This assumption changes (46c) to

$$T=(M/4+M_3/2)(\dot{l}_1^2 +l_1^2\dot{\theta}_1^2). \qquad (46d)$$

Now , we find the potential energy, using the formula

$$P=mgh \qquad (47a)$$

where h is the height and g the acceleration of gravity. Thus,

$$P_1 =Mg(-l_1 \sin\theta_1/2) \qquad (47b)$$

$$P_2 =Mg(-l_2 \sin\theta_2/2) \qquad (48)$$

$$P_3 =M_3 g(-l_1 \sin\theta_1) \qquad (49)$$

where from Eq. (38)

$$l_1 \sin\theta_1/2=l_2 \sin\theta_2/2 \ . \qquad (49a)$$

The total potential energy is

$$P=P_1+P_2+P_3=-(M+M_3)gl_1\sin\theta_1 \qquad (50)$$

We now combine Equations (46d) and (50) to produce the Lagrangian for this manipulator

$$L=T-P=(M/4+M_3/2)(\dot{l}_1^2+l_1^2\dot{\theta}_1^2)+(M+M_3)gl_1\sin\theta_1 \qquad (51)$$

The free-body diagram of the Link 1 is shown in Fig. 7. The total force applied on the system is

$$F=f_{m1}-f_{m2}\cos\theta-f_y\sin\theta_1 \qquad (52)$$

where $$\theta=\pi-(\theta_1+\theta_2) \ . \qquad (53)$$

Therefore,

$$F=f_{m1}+f_{m2}\cos(\theta_1+\theta_2)-f_y\sin\theta_1 \qquad (54)$$

Although there is not any torque about θ_1, but when the second link is extending or contracting, it makes the first one to rotate. So we can state that the forces f_{m2} and f_y apply a torque about θ_1 as the following:

$$T_\theta=f_{m2}\,l_1\sin\theta+f_y l_1\cos\theta_1 \qquad (55)$$

or

$$T_\theta=[f_{m2}\sin(\theta_1+\theta_2)+f_y\cos\theta_1]l_1 \qquad (56)$$

In Equations (55) and (56) f_{m1} is pushing and f_{m2} is pulling. Using Equation (32) we can find the forces applied by the linear actuators by considering

$$\frac{\partial L}{\partial \dot{l}_1} = (M/2+M_3)\dot{l}_1 \tag{57}$$

$$\frac{d}{dt}\frac{\partial L}{\partial \dot{l}_1} = (M/2+M_3)\ddot{l}_1 \tag{58}$$

$$\frac{\partial L}{\partial l_1} = (M/2+M_3)l_1\dot{\theta}_1^2 + (M+M_3)g\sin\theta_1 . \tag{59}$$

Therefore,

$$F = (M/2+M_3)\ddot{l}_1 - (M/2+M_3)l_1\dot{\theta}_1^2 - (M+M_3)g\sin\theta_1 \tag{60}$$

Similarly, from the torque

$$\frac{\partial L}{\partial \dot{\theta}_1} = (M/2+M_3)l_1^2\dot{\theta}_1 \tag{61}$$

$$\frac{d}{dt}\frac{\partial L}{\partial \dot{\theta}_1} = (M/2+M_3)(2l_1\dot{l}_1\dot{\theta}_1 + l_1^2\ddot{\theta}_1) \tag{62}$$

$$\frac{\partial L}{\partial \theta_1} = (M+M_3)gl_1\cos\theta_1 . \tag{63}$$

Thus,

$$T_\theta = (M/2+M_3)(2l_1\dot{l}_1\dot{\theta}_1 + l_1^2\ddot{\theta}_1) - (M+M_3)gl_1\cos\theta_1 \tag{64}$$

Substituting the values of F and T_θ from (54) and (56) into Equations (60) and (64) yield

$$f_{m1} + f_{m2}\cos(\theta_1+\theta_2) - f_y \sin\theta_1 = (M/2+M_3)\ddot{l}_1 - (M/2+M_3)l_1\dot{\theta}_1^2 - (M+M_3)g\sin\theta_1 \quad (65)$$

$$f_{m2}\sin(\theta_1+\theta_2) + f_y\cos\theta_1 = (M/2+M_3)l_1\ddot{\theta}_1 + (M/2+M_3)(2\dot{l}_1\dot{\theta}_1) - (M+M_3)g\cos\theta_1 \quad (66)$$

To write the above equations in terms of joint variables l_1 and θ_1, we must eliminiate θ_2. From trigonometry we obtain

$$\cos(\theta_1+\theta_2) = \cos\theta_1\cos\theta_2 - \sin\theta_1\sin\theta_2 \quad (67)$$

Substituting the values of $\cos\theta_2$ and $\sin\theta_2$ from Equations (37) and (38) into (67) we get

$$\cos(\theta_1+\theta_2) = \cos\theta_1[(d-l_1\cos\theta_1)/l_2] - \sin\theta_1[(l_1\sin\theta_1)/l_2] \quad (68)$$

or $$\cos(\theta_1+\theta_2) = (d\cos\theta_1 - l_1)/l_2 \ . \quad (69)$$

Similarly,

$$\sin(\theta_1+\theta_2) = \sin\theta_1\cos\theta_2 + \cos\theta_1\sin\theta_2 \quad (70)$$

or

$$\sin(\theta_1+\theta_2) = \sin\theta_1[(d-l_1\cos\theta_1)/l_2] + \cos\theta_1[(l_1\sin\theta_1)/l_2]$$
$$= d\sin\theta_1/l_2 \quad (71)$$

From Fig. 6, we obtain

$$l_2^2 = d^2 + l_1^2 - 2dl_1\cos\theta_1 \quad (72)$$

$$l_2 = (l_1^2 + d^2 - 2dl_1\cos\theta_1)^{1/2} \quad (73)$$

Substituting l_2 into Equations (69) and (71)

$$\cos(\theta_1+\theta_2)=\frac{d\cos\theta_1-l_1}{(l_1^2+d^2-2dl_1\cos\theta_1)^{1/2}} \qquad (74)$$

$$\text{and } \sin(\theta_1+\theta_2)=\frac{d\sin\theta_1}{(l_1^2+d^2-2dl_1\cos\theta_1)^{1/2}} \qquad (75)$$

Equations (65) and (66) can be rewritten as

$$f_{m1}+f_{m2}a(t)-f_y\sin\theta_1=K_1\ddot{l}_1-K_1l_1\dot{\theta}_1^2-K_2g\sin\theta_1 \qquad (76)$$

$$f_{m2}b(t)+f_y\cos\theta_1=K_1\ddot{\theta}_1+2K_1\dot{l}_1\dot{\theta}_1-K_2g\cos\theta_1 \qquad (77)$$

where

$$K_1=M/2+M_3 \quad ; K_2=M+M_3 \qquad (78)$$

$$a(t)=(d\cos\theta_1-l_1)/c(t) \quad ; b(t)=d\sin\theta_1/c(t);$$

$$c(t)=(l_1^2+d^2-2dl_1\cos\theta_1)^{1/2} \quad . \qquad (79)$$

and f_{m1} and f_{m2} are actuator forces. The force f_y is the reaction force produced through contact with the reaction surface and is modelled as follows:

$$f_y=\begin{cases}-K_E(y-y_E) & \text{when in contact} \quad (y-y_E)<0\\ 0 & \text{otherwise} \quad (y-y_E)\geq 0\end{cases}$$

where y_E and K_E denote the position and stiffness of the reaction surface, respectively [3]. The consant K_E is

typically of the order of 10^6 N/m for a stiff environment.

The term $2K_1 l_1 \dot{\theta}_1$ in Eq. (77) represents the Coriolis force acting on Link 2 due to the Coriolis effect (when a mass particle m moves at a velocity of V relative to a moving coordinate frame rotating at an angular velocity w, the mass particle has the so-called Coriolis force given by 2m(wxV)). The last term $K_2 g \sin\theta_1$ and $K_2 g \cos\theta_1$ in Equations (76) and (77) accounts for the effect of gravity. The second term on the right side of Eq. (76) which is proportional to the square of the joint velocities shows the centrifugal force.

ii) Newton-Euler Method

In order to reduce the computation time for the simulation of the robot system, the equations of motion in terms of the Cartesian variables X and Y are needed. Fig. 8 illustrates the free body diagram of each link of the robot system. Applying Newton formulation for IEE, we obtain

$$F_{1x} + F_{2x} = M_3 \ddot{x} \qquad (81)$$

$$-F_{1y} + F_{2y} - M_3 g + f_y = M_3 \ddot{y} \qquad (82)$$

Knowing that $\dot{V}_{C1} = \dot{V}_{C2} = \dot{V}_P / 2$, for Links 1 and 2 we can write

$$f_{m1}\cos\theta_1 - F_{1x} = M\ddot{x}/2 \tag{83}$$

$$-f_{m1}\sin\theta_1 + F_{1y} - Mg = M\ddot{y}/2 \tag{84}$$

$$f_{m2}\cos\theta_2 - F_{2x} = M\ddot{x}/2 \tag{85}$$

$$f_{m2}\sin\theta_2 - F_{2y} - Mg = M\ddot{y}/2 \tag{86}$$

Substituting the values of F_{1x} and F_{2x} from Equations (83) and (85) into (81) and F_{1y}, F_{2y} from (84) and (86) into (82), and using the relations of (35) and (36), we obtain

$$f_{m1}(x/l_1) + f_{m2}[(d-x)/l_2] = K_2\ddot{x} \tag{87}$$

$$f_{m1}(y/l_1) - f_{m2}(y/l_2) + f_y = K_2\ddot{y} + K_3 g \tag{88}$$

where $$K_3 = 2M + M_3 \tag{89}$$

and l_1, l_2, x and y are related through Equations (7) and (8).

5.3 HYBRID CONTROL OF THE 2-DEGREE-OF-FREEDOM ROBOT

The block diagram of the hybrid control system is shown in Fig. 9. Both position and velocity feedback are employed to improve the response. We assume that the robot is to move from the initial position $x_i = A$, $y_i = B$ to the final position $x_f = x_d$, while exerting a force $f_{dy} = f_0$ in

the vertical direction. Manipulator is moving in a horizontal plane so that gravity may be ignored [6]. The desired velocity in X direction will be $\dot{x}_d = 0_1$ while in y direction is zero.

5.3.1 POSITION AND VELOCITY CONTROL

For a 2-degree-of-freedom robot the selection matrix defined in Eq.(1), will be

$$S_{jj} = \begin{bmatrix} 1 & 0 \\ 0 & 1 \end{bmatrix}$$

Since we are interested in controlling position in x direction ($s_{11}=0$), and force in Y direction ($s_{22}=1$), the corresponding compliance matrix is $S = \begin{bmatrix} 0 & 0 \\ 0 & 1 \end{bmatrix}$

$$\text{and } [I]-[S] = \begin{bmatrix} 1 & 0 \\ 0 & 1 \end{bmatrix} - \begin{bmatrix} 0 & 0 \\ 0 & 1 \end{bmatrix} = \begin{bmatrix} 1 & 0 \\ 0 & 0 \end{bmatrix} \qquad (90)$$

where [I] is the identity matrix. The position error is

$$\Delta X(t) = X_d - \Lambda(q(t)) = \begin{bmatrix} x_d \\ y_d \end{bmatrix} - \begin{bmatrix} x(t) \\ y(t) \end{bmatrix} = \begin{bmatrix} A \\ B \end{bmatrix} - \begin{bmatrix} x(t) \\ y(t) \end{bmatrix} = \begin{bmatrix} A-x(t) \\ B-y(t) \end{bmatrix} \qquad (91)$$

This error is mapped into the position controlled subspace. The compliance matrix S serves as a mask to separate the force controlled and position controlled degrees of freedom. The Cartesian error signals are obtained as

$$X_e(t) = \begin{bmatrix} x_e(t) \\ y_e(t) \end{bmatrix} = \{[I]-[S]\}\Delta X(t) = \begin{bmatrix} 1 & 0 \\ 0 & 0 \end{bmatrix} \begin{bmatrix} A-x(t) \\ B-y(t) \end{bmatrix} = \begin{bmatrix} A-x(t) \\ 0 \end{bmatrix} \qquad (92)$$

Transforming them back into the joint space, we find the corresponding joint variables errors. Since X_e is a differential change, we can use the Jacobian to find the corresponding (approximate) differential change in the vector of joint variables

$$q(t)=\begin{bmatrix} l_1(t) \\ l_2(t) \end{bmatrix}$$

Recalling J from Equation (24) we find its inverse as follows:

$$J^{-1} = \frac{Adj[J]}{Det|J|} \qquad (93a)$$

where

$$Adj|J| = \begin{bmatrix} \frac{l_2(d^2+l_1^2-l_2^2)}{d\Theta} & \frac{l_2}{d} \\ -\frac{l_1(d^2+l_2^2-l_1^2)}{d\Theta} & \frac{l_1}{d} \end{bmatrix} \qquad (93b)$$

and

$$Det|J| = \frac{l_1}{d}\left[\frac{l_2(d^2+l_1^2-l_2^2)}{d\Theta}\right] + \frac{l_2}{d}\left[\frac{l_1(d^2+l_2^2-l_1^2)}{d\Theta}\right] \qquad (93c)$$

$$Det|J| = \frac{l_1 l_2(d^2+l_1^2-l_2^2+d^2+l_2^2-l_1^2)}{d^2\Theta} \qquad (93d)$$

or

$$Det|J| = \frac{2l_1 l_2}{\Theta} \qquad (93e)$$

Therefore,

$$J^{-1}=\begin{bmatrix} \dfrac{l_1^2-l_2^2+d^2}{2l_1d} & \dfrac{[4d^2l_1^2-(l_1^2-l_2^2+d^2)^2]^{1/2}}{2l_1d} \\ \dfrac{-(l_2^2-l_1^2+d^2)}{2l_2d} & \dfrac{[4d^2l_1^2-(l_1^2-l_2^2+d^2)^2]^{1/2}}{2l_2d} \end{bmatrix} \tag{94}$$

For simplicity, we define

$$J^{-1}=\begin{bmatrix} E_1 & E_2 \\ E_3 & E_4 \end{bmatrix} \tag{95}$$

where E_i's are given in Equation (94). Thus

$$q_e(t)=\begin{bmatrix} l_{e1}(t) \\ l_{e2}(t) \end{bmatrix}=J^{-1}X_e(t) \tag{96}$$

$$q_e(t)=\begin{bmatrix} E_1 & E_2 \\ E_3 & E_4 \end{bmatrix}\begin{bmatrix} A-x(t) \\ 0 \end{bmatrix}=\begin{bmatrix} E_1[A-x(t)] \\ E_3[A-x(t)] \end{bmatrix} \tag{97a}$$

The error in joint variables will be

$$l_{e1}(t)=E_1[A-x(t)] \tag{97b}$$

$$l_{e2}(t)=E_3[A-x(t)] \tag{97c}$$

Applying the same method for velocity control, we find

$$\Delta\dot{X}(t)=\dot{X}_d-\dot{A}(q(t))=\begin{bmatrix} \dot{x}_d \\ \dot{y}_d \end{bmatrix}-\begin{bmatrix} \dot{x}(t) \\ \dot{y}(t) \end{bmatrix}=\begin{bmatrix} 0 & -\dot{x}(t) \\ 1 & \\ 0 & -\dot{y}(t) \end{bmatrix} \tag{98}$$

$$\dot{X}_e(t)=\begin{bmatrix} \dot{x}_e(t) \\ \dot{y}_e(t) \end{bmatrix}=\begin{bmatrix} 1 & 0 \\ 0 & 0 \end{bmatrix}\begin{bmatrix} 0 & -\dot{x}(t) \\ 1 & \\ 0 & -\dot{y}(t) \end{bmatrix}=\begin{bmatrix} 0 & -\dot{x}(t) \\ 1 & \\ 0 & \end{bmatrix} \tag{99}$$

$$\dot{q}_e(t)=\begin{bmatrix}\dot{l}_{el}(t)\\ \dot{l}_{e2}(t)\end{bmatrix}=J^{-1}\dot{X}_e(t) \qquad (100a)$$

$$\dot{q}_e(t)=\begin{bmatrix}E_1 & E_2\\ E_3 & E_4\end{bmatrix}\begin{bmatrix}\theta_1-\dot{x}(t)\\ 0\end{bmatrix}=\begin{bmatrix}E_1[\theta_1-\dot{x}(t)]\\ E_3[\theta_1-\dot{x}(t)]\end{bmatrix} \qquad (100b)$$

Therefore, the error in joint velocities will be

$$\dot{l}_{el}(t)=E_1[\theta_1-\dot{x}(t)] \qquad (100c)$$

$$\dot{l}_{e2}(t)=E_3[\theta_1-\dot{x}(t)] \qquad (100d)$$

To move the joints and reduce the error, we use PD (proportional derivative) controller for position. Thus,

$$u_p=q_e(t)[K_{rp}] \qquad (101a)$$

$$v_p=\dot{q}_e(t)[K_{rpd}] \quad . \qquad (101b)$$

The error in lengths due to the error in position and velocity are

$$u_{rp}(t)=u_p(t)+v_p(t) \qquad (102a)$$

For Link 1 we get

$$u_{rpl}(t)=l_{el}(t)K_{rpl}+\dot{l}_{el}(t)K_{rpdl} \qquad (102b)$$

and for Link 2

$$u_{rp2}(t)=l_{e2}(t)K_{rp2}+\dot{l}_{e2}(t)K_{rpd2} \qquad (102c)$$

Substituting the values of l_{el}, l_{e2}, $\dot{l}_{el}$, and $\dot{l}_{e2}$ into (102b) and (102c), we obtain

$$u_{rpl}(t)=E_1(A-x(t))K_{rpl}+E_1(\theta_1-\dot{x}(t))K_{rpdl} \qquad (103a)$$

$$u_{rp2}(t)=E_3(A-x(t))K_{rp2}+E_3(\theta_1-\dot{x}(t))K_{rpd2} \qquad (103b)$$

5.3.2 FORCE CONTROL

Knowing the desired force

$$F_d = \begin{bmatrix} f_{dx} \\ f_{dy} \end{bmatrix} = \begin{bmatrix} 0 \\ f_0 \end{bmatrix}$$

and the actual force $F(t)=\begin{bmatrix} f_x \\ f_y \end{bmatrix}$, the force error is computed as

$$\Delta F(t)=F_d(t)-F(t)=\begin{bmatrix} 0 \\ f_0 \end{bmatrix}-\begin{bmatrix} f_x(t) \\ f_y(t) \end{bmatrix}=\begin{bmatrix} -f_x(t) \\ f_0-f_y(t) \end{bmatrix} \qquad (104)$$

Note that the coordinate system is parallel to the constraint frame. So, the force transformation matrix is

$$\begin{bmatrix} 1 & 0 \\ 0 & 1 \end{bmatrix}$$

The Cartesian error signal is computed by

$$F_e(t)=\begin{bmatrix} f_{xe} \\ f_{ye} \end{bmatrix} = [S]\Delta F(t) \qquad (105a)$$

$$F_e(t)=\begin{bmatrix} 0 & 0 \\ 0 & 1 \end{bmatrix}\begin{bmatrix} -f_x(t) \\ f_0-f_y(t) \end{bmatrix}=\begin{bmatrix} 0 \\ f_0-f_y(t) \end{bmatrix} \qquad (105b)$$

The corresponding Joint space error is found by

$$\tau_e(t)=J^T F_e(t) \qquad (106)$$

where $\tau_e(t)=\begin{bmatrix} f_{re1} \\ f_{re2} \end{bmatrix}$ and J^T is the Jacobian transpose that is derived as

$$J^T = \begin{bmatrix} \frac{l_1}{d} & \frac{l_1(d^2+l_2^2-l_1^2)}{d\theta} \\ \frac{-l_2}{d} & \frac{l_2(d^2+l_1^2-l_2^2)}{d\theta} \end{bmatrix} \qquad (107)$$

For simplicity, we define $J^T = \begin{bmatrix} G_1 & G_2 \\ G_3 & G_4 \end{bmatrix}$ (108)

then

$$\tau_e(t) = \begin{bmatrix} G_1 & G_2 \\ G_3 & G_4 \end{bmatrix} \begin{bmatrix} 0 \\ f_0 - f_y \end{bmatrix} = \begin{bmatrix} G_2(f_0 - f_y) \\ G_4(f_0 - f_y) \end{bmatrix} \qquad (109a)$$

or

$$f_{rel}(t) = G_2(f_0 - f_y) \qquad (109b)$$

$$f_{re2}(t) = G_4(f_0 - f_y) \qquad (109c)$$

For force control, we will use PE (proportional error) controller. Therefore, the error in lengths due to the error in force will be

$$u_{rf} = K_{rf} f_{re} \qquad (110a)$$

or

$$u_{rf1}(t) = K_{rf1} f_{rel}(t) = K_{rf1} G_2(f_0 - f_y(t)) \qquad (110b)$$

$$u_{rf2}(t) = K_{rf2} f_{re2}(t) = K_{rf2} G_4(f_0 - f_y(t)) \qquad (110c)$$

Finally the inputs to the linear actuators are computed by

$$e_{al}(t)=u_{rpl}+u_{rfl}=E_1(A-x(t))K_{rpl}+E_1(Q_1-\dot{x}(t))K_{rpdl}+G_2(f_0-f_y(t))K_{rfl} \quad (111)$$

$$e_{a2}(t)=u_{rp2}+u_{rf2}=E_3(A-x(t))K_{rp2}+E_3(Q_1-\dot{x}(t))K_{rpd2}+G_4(f_0-f_y(t))K_{rf2} \quad (112)$$

5.3.3 LINEAR ACTUATOR DYNAMICS

Since no transient analysis of DC linear motor is available, we assume that its dynamics is identical to that of DC motor. By neglecting the armature inductance and the load torque, the transfer function between the motor actuating force and the input voltage e_a is obtained by [27]

$$\frac{F_m(S)}{E_a(S)}=\frac{K_i K_m(J_m S+B_m)}{R_a(J_m S+B_m)+K_i K_b} \quad (113)$$

where we assumed that $F_m(S)=K_m T_m(S)$ and

R_a =armature resistance

J_m =rotor inertia of motor

K_b =back emf constant

K_i =torque constant

B_m =viscous frictional coefficient

6. SIMULATION

In order to examine the behavior of the proposed hybrid controller, we conducted several simulation runs of the system. The robot dynamics and the hybrid control scheme are simulated using the System Simulation Language (SYSL) developed by E^2 Consulting for the IBM PC.

6.1 RESULTS AND DISCUSSION

Fig. 10 shows the responses of the system that was controlled to stay at a fixed position X =10 cm, Y =-10 cm while mainting a constant force F =90 N. The responses had small overshoots in vertical force and position, which is caused by the initial forces of the motors (f_{m1} and f_{m2} =6N). The settling time was about 0.1 sec. The error in the horizontal position was about 10^{-4} cm and was not recorded in the graph.

Figures 11 and 12 depict the responses of the robot controlled to move from X =0 to X =1 cm horizontally while keeping a constant force F =90 N on the reaction surface. The response shows that the robot reached the destination in 0.5 sec in an "overdamped" fashion. The average velocity in Fig. 11 is 8 cm/sec and in Fig. 12 7cm/sec. The first case shows higher overshoot but faster

response. The vertical force and position were settled after about 0.1 sec with relatively small overshoots.

Figures 13 and 14 demonstrate the control of force in the presence of position disturbances. The controller attempts to maintain a constant 90 N force at a fixed horizontal position on the reaction table while the table is moving away from the robot in y direction at a constant rate 0.1 cm/sec (Fig. 13), and 0.08 cm/sec (Fig.14). The quality of the force was quite good while there was some disturbance in the horizontal position (about 0.01 cm error). When the surface stops moving (after 1 sec), control returns to a stable steady state. At the end of the ramp where there are acceleration there was a little disturbance in the force. In these figures, we note that the vertical position follows the movement of the table closely.

In all simulation runs, the controller gains, actuator parameters and robot masses are adjusted until a stable response with little overshoots is achieved. Controller feedback gains and the numerical values of parameters used in simulation are given below

K_{rp1} =39. N/m K_{rp2} =25. N/m

K_{rpd1} =K_{rpd2} =25. N/m K_{rf1} =K_{rf2} =0.3

M=3. Kg M_3 =3.5 kg

$K_E = 9 \times 10^5$ N/m $d = 23$ cm

$l_1 = l_2 = 15$ cm

7. CONCLUSIONS

In this report the hybrid control was proposed to control the compliance of the existing NASA robot. A study of coordinate transformation of the IEE showed that its forward kinematic problem does not have a closed-form solution and consists of non-linear equations which Newton-Raphson's method was employed to solve it.

The kinematics, dynamics and hybrid controller of the 2-degree-of-freedom robot were presented and its simulation results were discussed.

Even though we obtained some good results, no clear relationship between the controller gains and system responses have been obtained. Further research can focus on the development of a guideline to select controller gains for stable and responsive robot systems.

References

1. NASA, "Advancing Automation and Robotics Technology for the Space Statation and for the U.S. Economy," Vol. II, NASA TM 87566, Advance Technology Advisory Committee, March 1985.

2. Paul, Richard P.c. and Shimano, Bruce, " Compliance and Control," Robot Motion , Planning and Control , Brady , M. et al, eds, M.I.T. Press, Cambridge, Mass., 1983.

3. Asada, H. and Slotine J., Robot Analysis and Control , Wiley & Sons, 1986

4. Whitney, Daniel E., " Force Feedback Control of Manipulator Fine Motions", ASME, Journal of Dynamic Systems, Measurement,and Control, June 1977.

5. Mason , M.T. , " Compliance and Force Control for Computer Controlled Manipulators", IEEE Trans. Systems , Man, Cybernetics, SMC-11, P.418, 1981.

6. Snyder, Wesley E., Industrial Robots: Computer Interfacing and Control, Prentice Hall, Englewood Cliffs , New Jersey, 1985.

7. Rairbert ,M.H. and Craig, J.J., "Hybrid Position/Force Control of Manipulators ," ASME, Journal of Dynamic Systems, Measurement and Control , 102 , pp. 126-133, June 1981.

8. Premack, Timothy et al ,"Design and Implementation of a Compliant Robot with Force Feedback and Strategy Planning Software " NASA, Tech. Memo. 86111, GSFC, May 1984.

9. Critchlow, Arthur J. , Introduction to Robotics, Macmillan Publishing Co.,New York 1985.

10. Nguyen, Charles C. and Premack, Timothy, "Active Compliant Control of Robot Manipulators", NASA Report ,NASA/GSFC, July 1985.

11. Saridis, G. N., Advances in Automation and Robotics ,Vol. 1, JAI Press Inc., Greenwich,Connecticut 1985.

12. Mason, M.T. , " Compliant Motion" Robot Motion , Planning,and Control,Brady M. et al,eds,M.I.T. Press , Cambridge,Mass., 1983.

13. Paul, Richard P., Robot Manipulators : Mathematics, Programming, and Control, The M.I.T. Press, Cambridge, Mass., 1981.

14. Whitney, L.E. ,"Quasi-Static Assembly of Compliantly Supported Rigid Parts " Robot Motion , Planning and Control, Brady M. et al, eds, M.I.T. Press, Cambridge, Mass., 1983.

15. Craig, John J.,Introduction to Robotics,Addison-Wesley ,1986.

16. Dieudonne, J. E. et al , " An Actuator Extension Transformation for a Motion Simulator and an Inverse Transformation Applying Newton-Raphson's Method" NASA Technical Note, NASA TN D-7067, November 1972.

17. Ortega, J.M. and Rheinboldt , W.c., Iterative Solution of Nonlinear Equations in several variables, Academic Press Inc.,New York, 1970.

18. Chua, L.O. and Wang, N.N.,"A New Approach to Overcome the Overflow Problem in Computer-Aided Analysis of Nonlinear Resistive Circuits," Int. Journal of Circuit Theory and Applications, Vol. 4, 1976.

19. Chua, L.O. and Pen-Min , L., Computer-Aided Analysis of Electronic Circuits, Prentice Hall,New Jersey,1975.

20. Dorf, Richard C.,Robotics and Automated Manufacturing , Reston Publishing Co., Reston, Virginia 1983.

21. Schiehlen, W. O. and Kreuzer, E. J., " Symbolic Computerized Derivation of Equations of Motion " , Dynamics of Multibody Systems , 1977.

22. Kazerooni, H. and Sheridan, T.B., "Robust Compliant Motion for Manipulators", IEEE Journal of Robotics and Automation, Vol. Ra-2 , June 1986.

23. Tanner, William R., Industrial Robots , Vol. 1, SME, Dearborn, Michigan, 1981.

24. Kuntz, H. B. and Jacubasch, A. H.,"Control Algorithms for Stiffening an Elastic Industrial Robot", IEEE Journal of Robotics and Automation, June 1985.

25. Luo, G. L. and Saridis , G.N., " L-Q Design of PID Controllers for Robot Arms", IEEE Journal of Robotics and Automation, No. 3, September 1985.

26. Jurica ,K.E. and Kuhn ,W. ," A Variable Configuration Controller for a Multipurpose Articulated End Effector ", NASA Report, Johnson Space Center, Houston, TX 1985.

27. Kuo, Benjamin C. ,Automatic Control Systems,Prentice Hall , Englewood Cliffs , New Jersey, 1982.

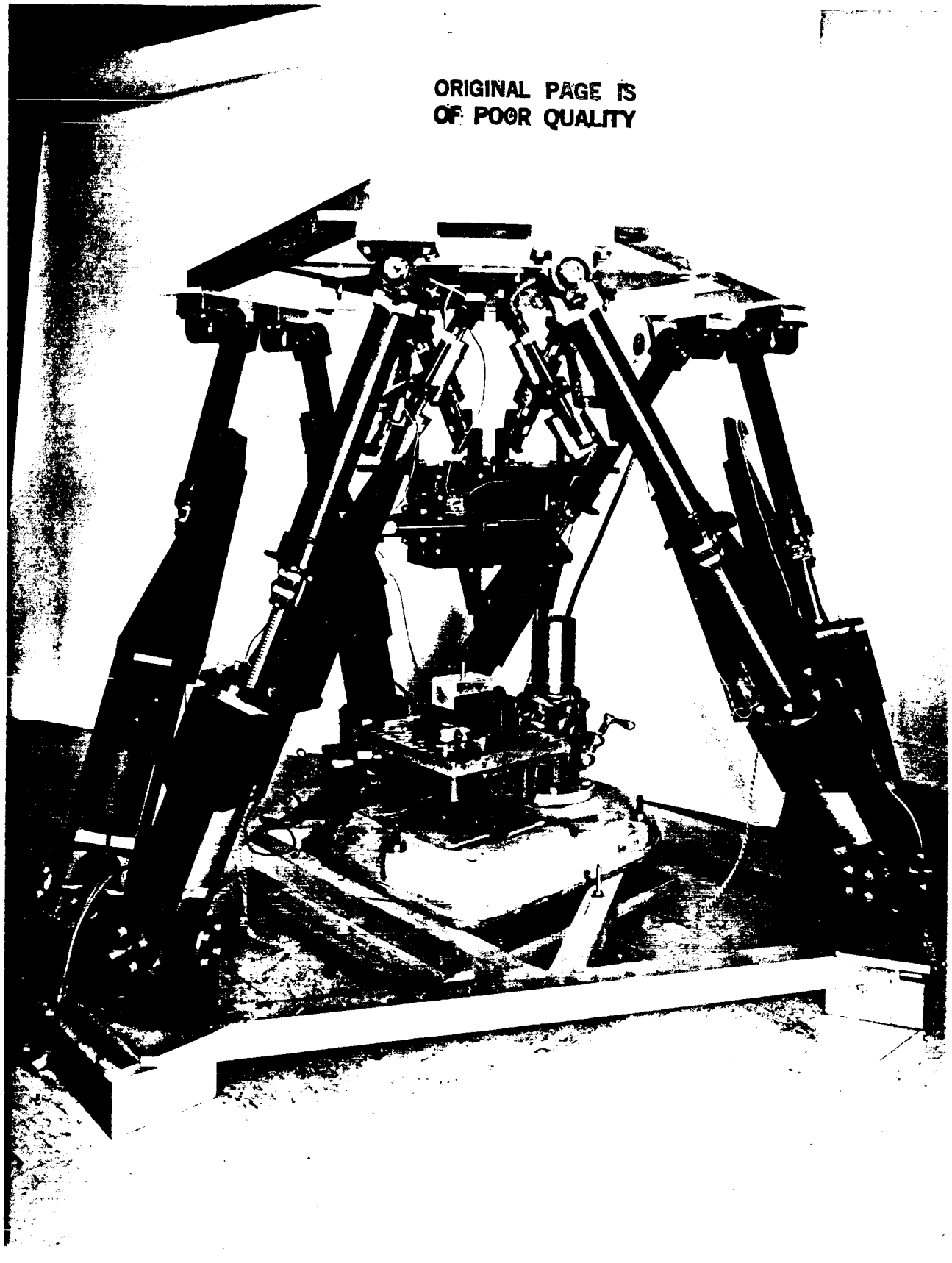

Fig. 1A : The NASA Passive Compliant Robot System

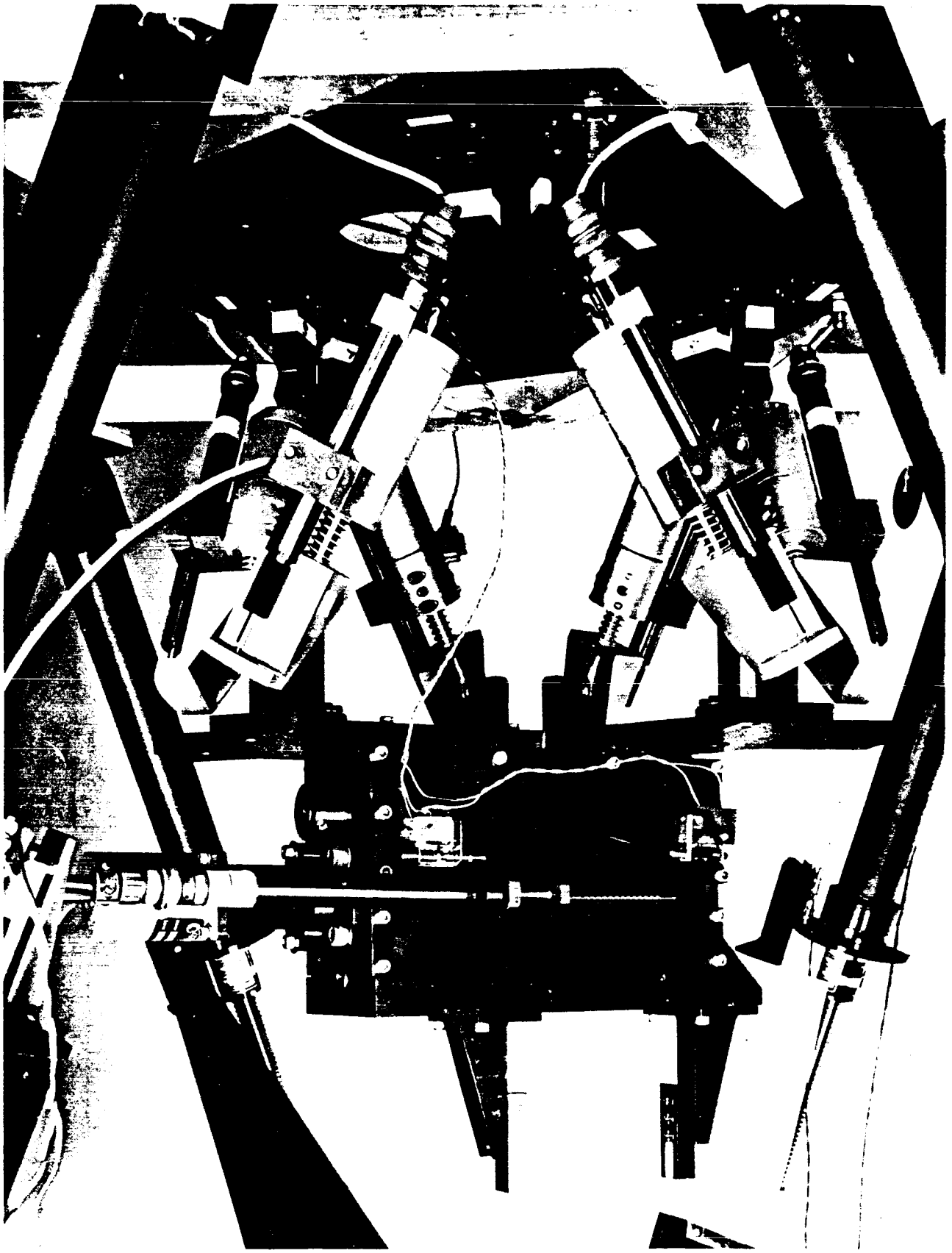

Fig. 1B : The Passive Compliant Platform

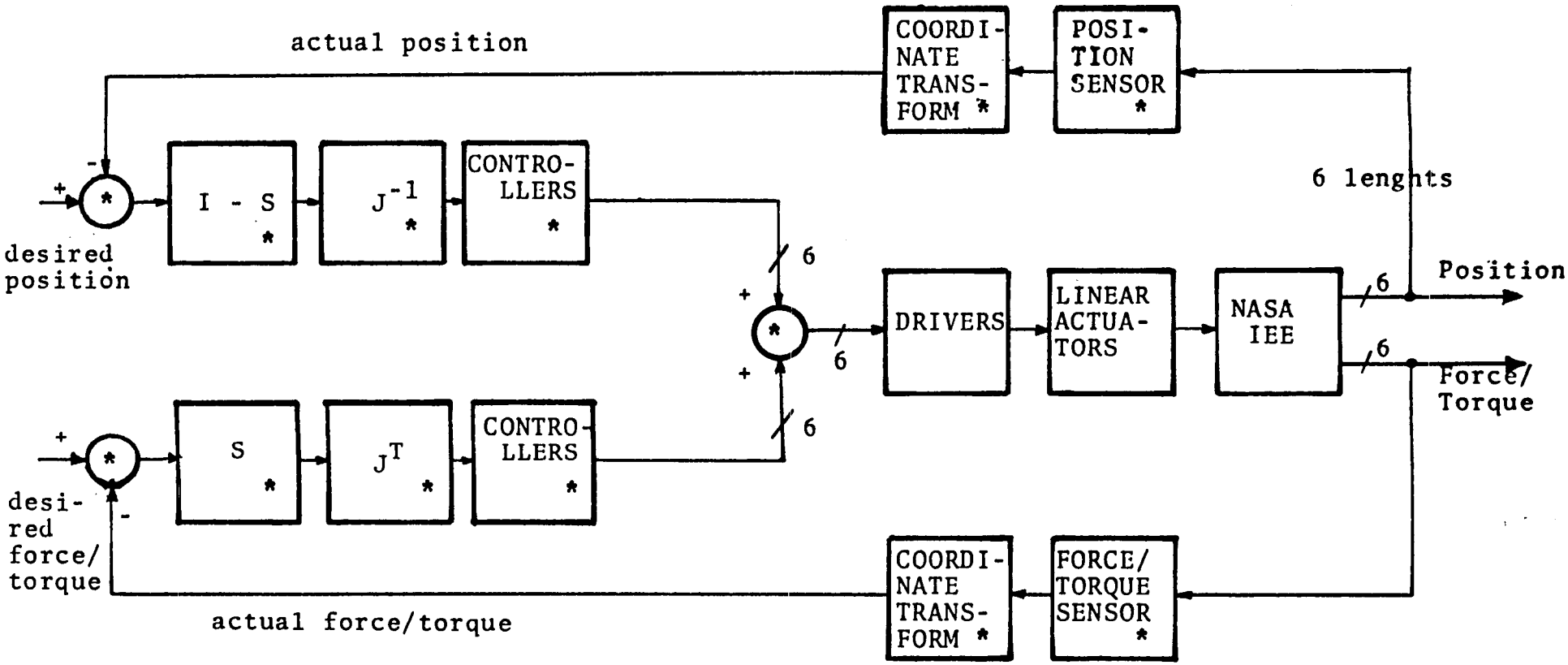

*:Implementation requires software
J=Jacobian Matrix
S=Compliance Selection Matrix

Fig. 2: The Hybrid Control Scheme

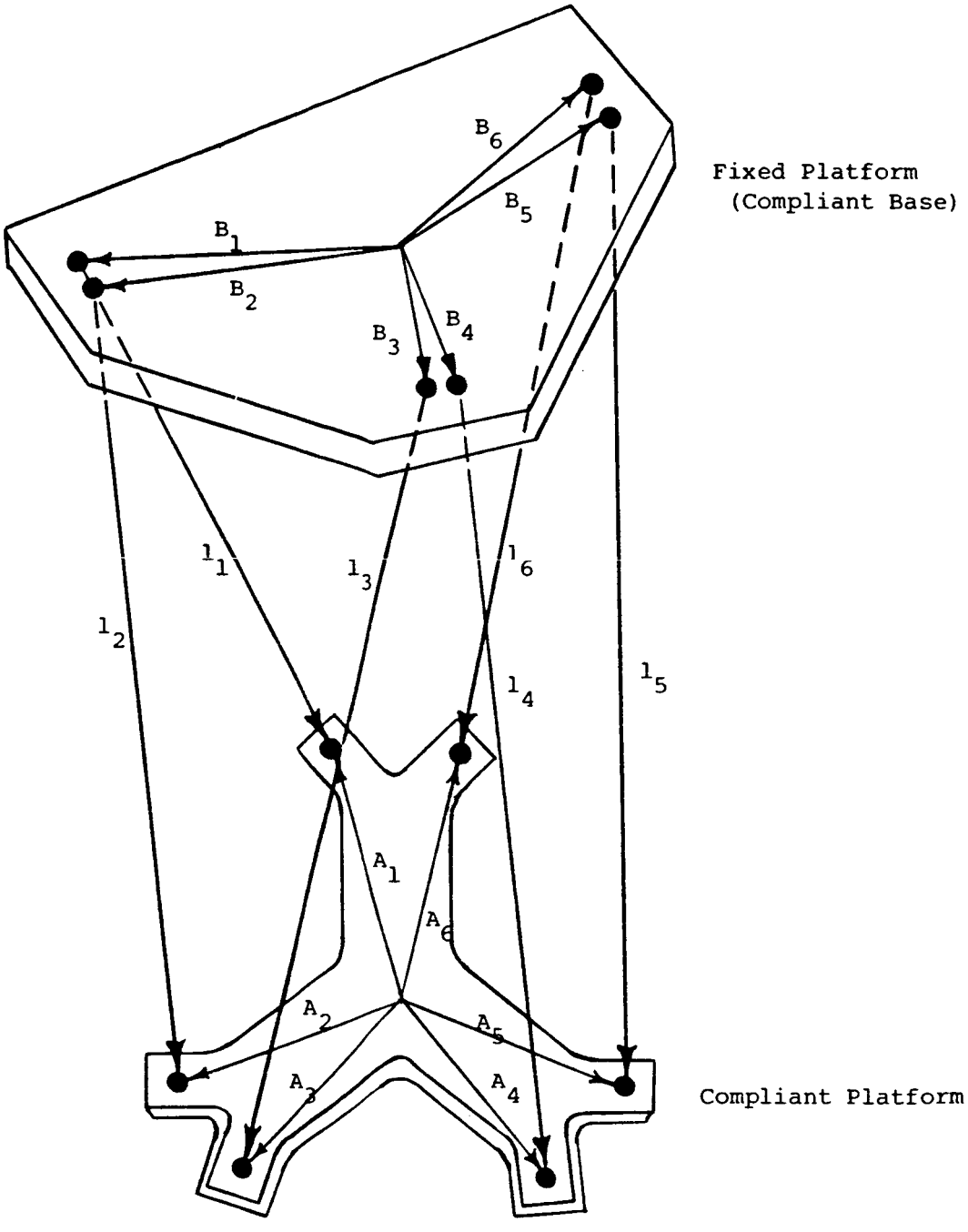

Fig. 3: Particular Orientation of Robot

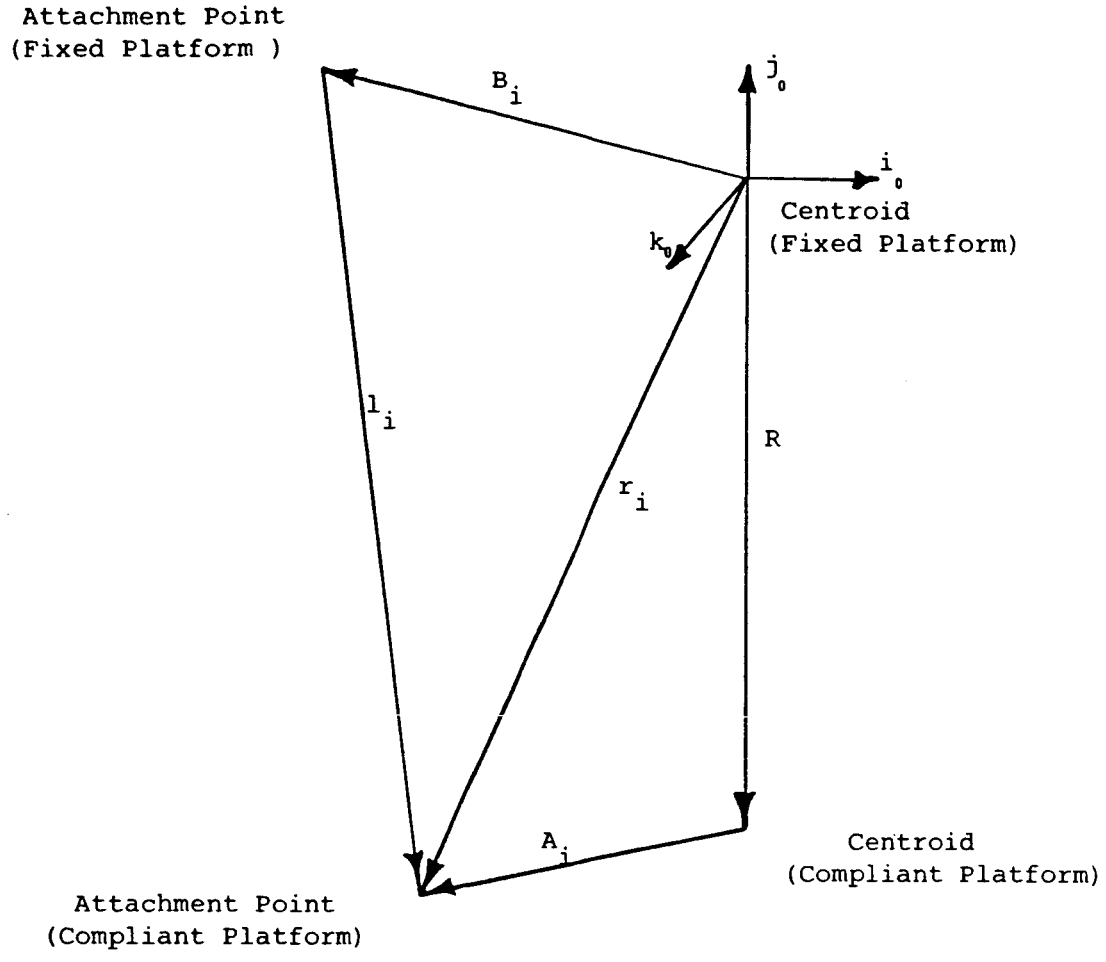

Fig. 4: Vector Relationships for Actuator i

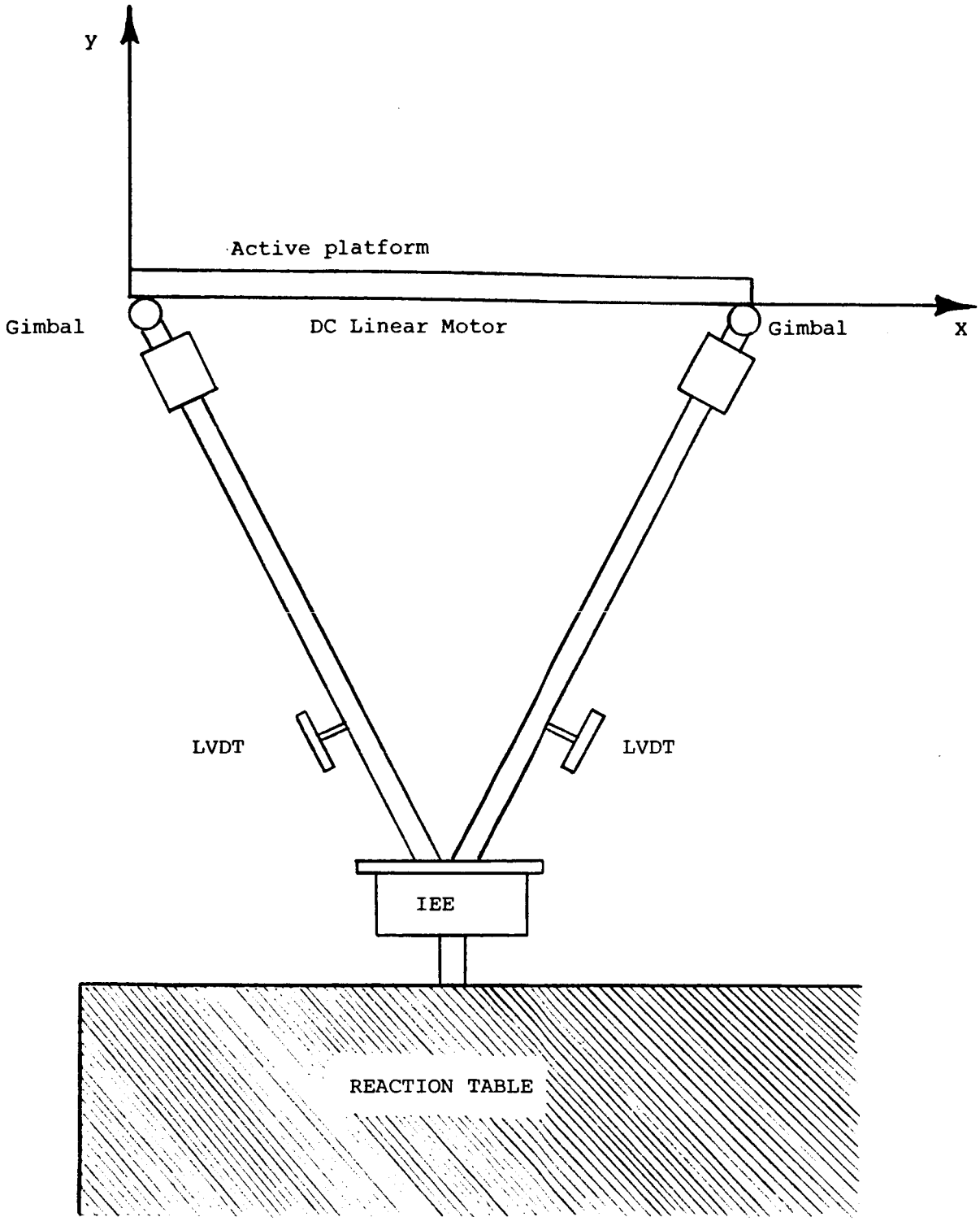

Fig. 5: The 2-Degree-of-Freedom Robot

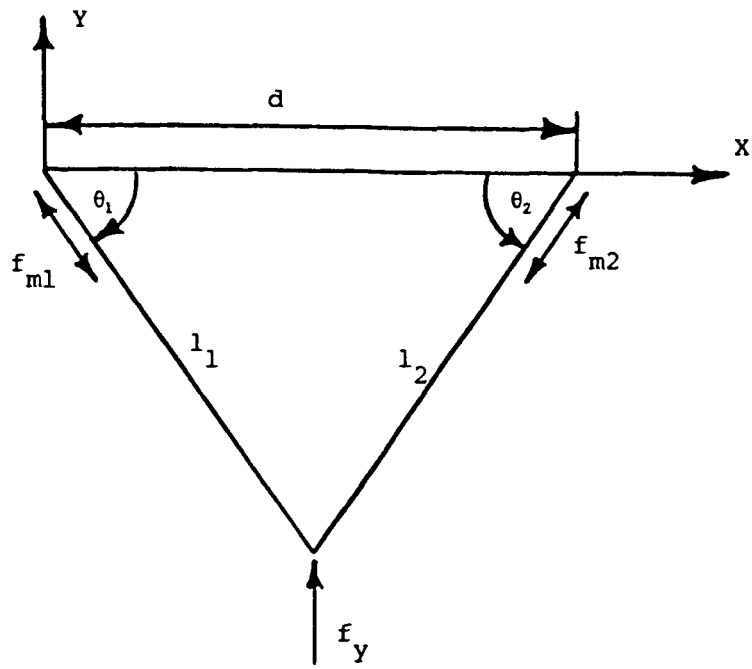

Fig. 6 : Forces Acting on the Robot

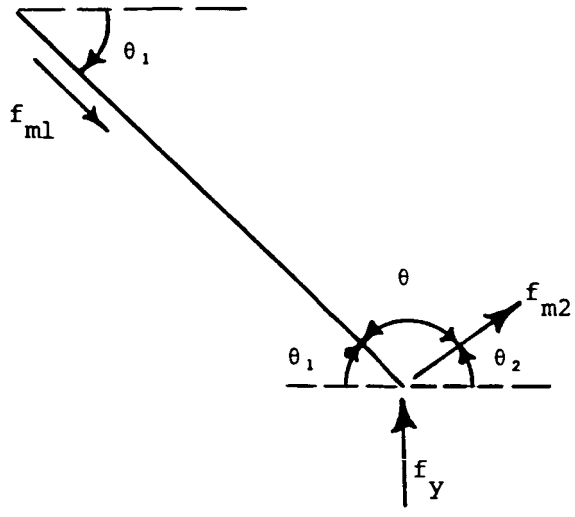

Fig. 7: The Free-Body Diagram of Link 1

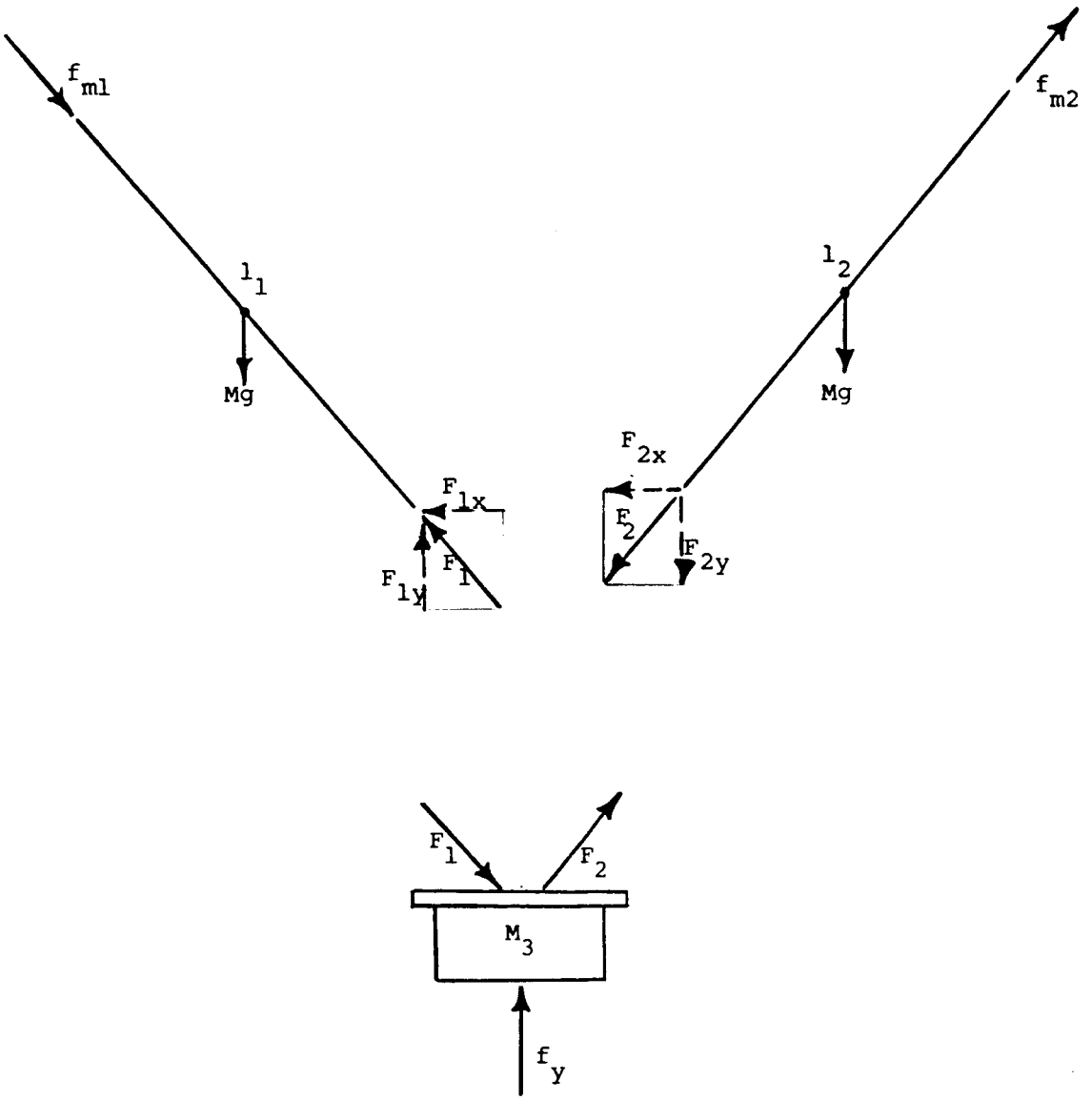

Fig. 8: The Free-Body Diagram

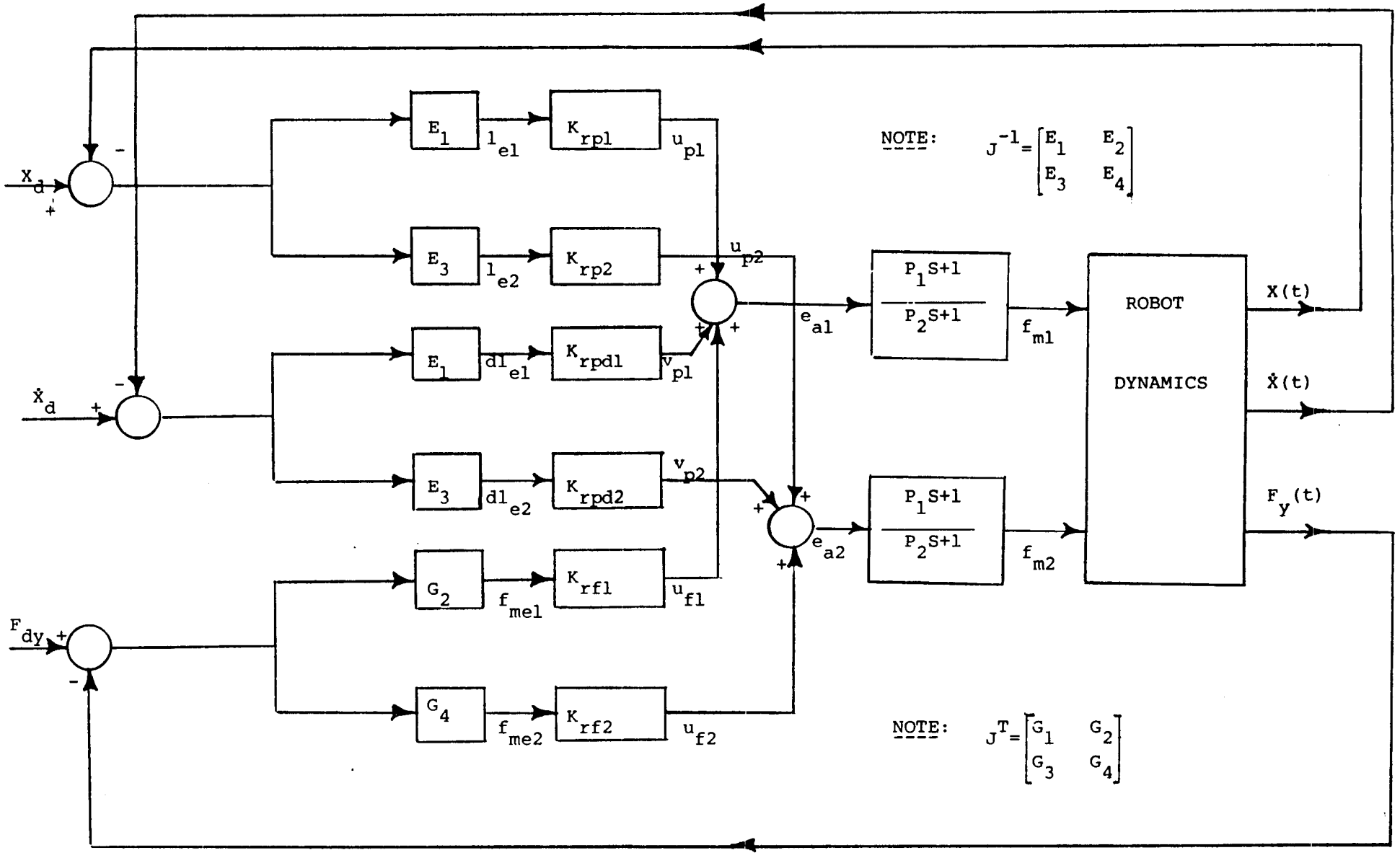

Fig. 9 : Implementation of the Hybrid Control Scheme for the 2-Degree-of-Freedom Robot.

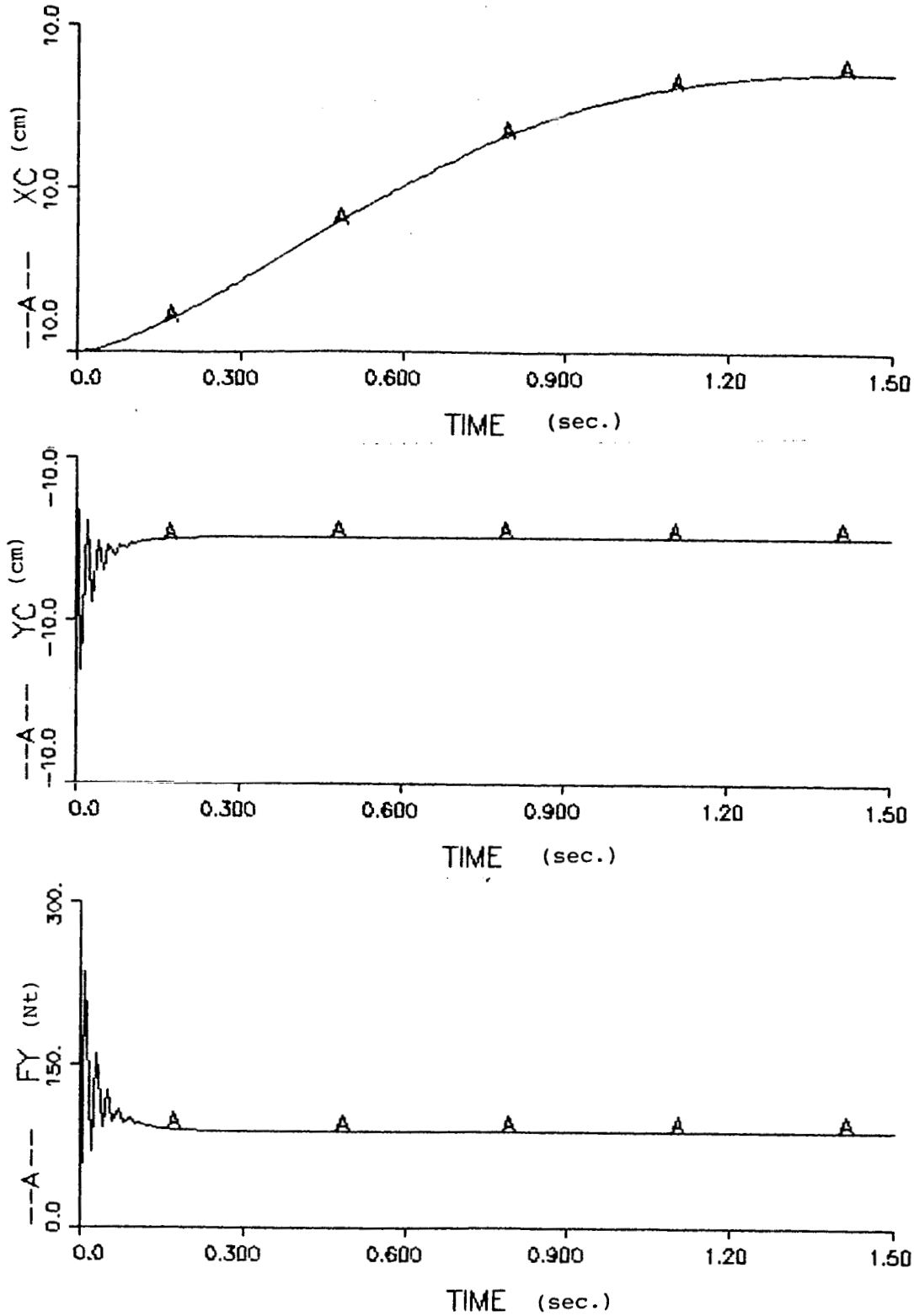

Fig. 10: Responses of the Robot for Control of Constant Force and Fixed Position

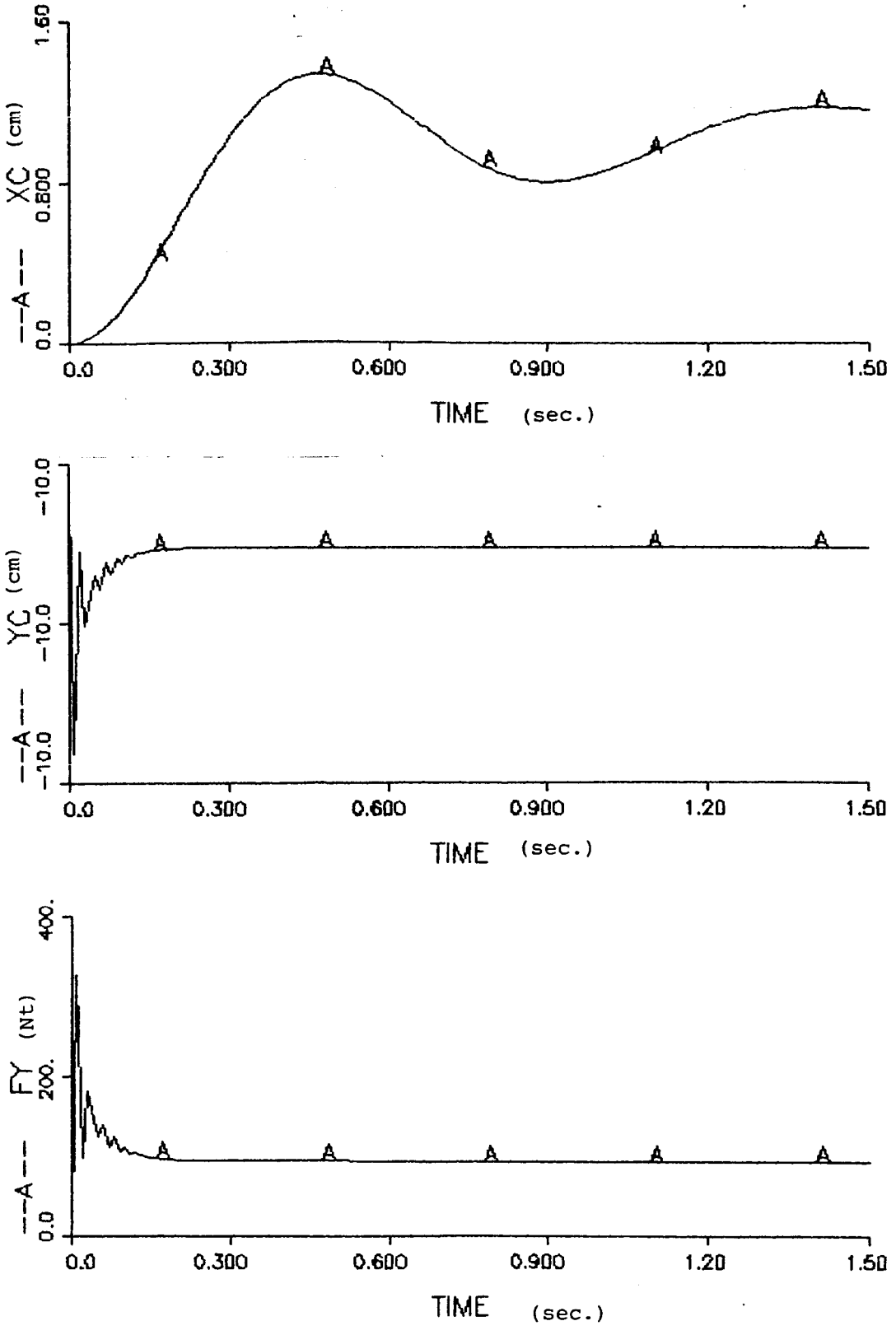

Fig. 11: Responses for Control of Constant Force while Moving on Horizontal Plane (V= 8. cm/sec)

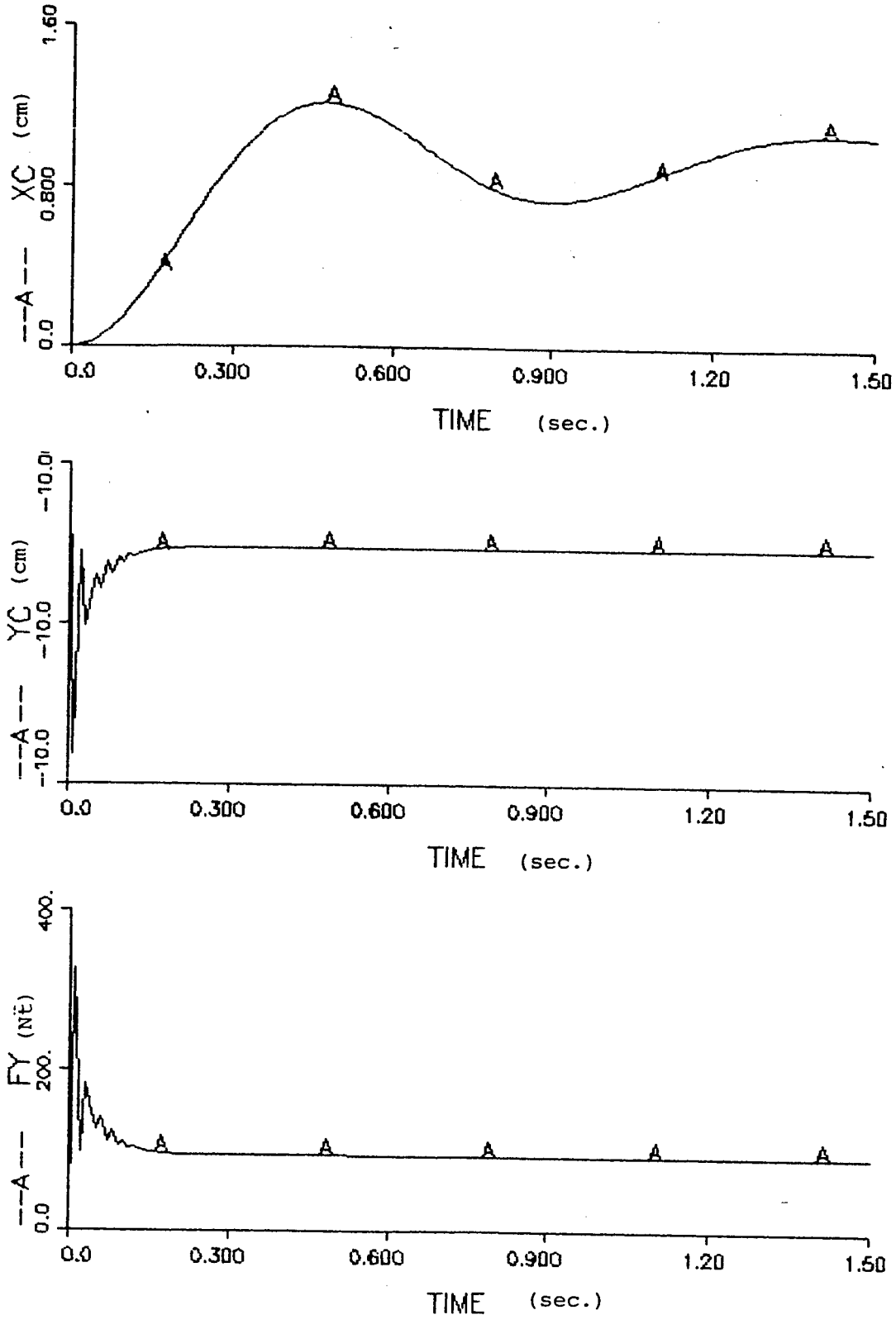

Fig. 12: Responses for Control of Constant Force while Moving on Horizontal Plane (V= 7. cm/sec)

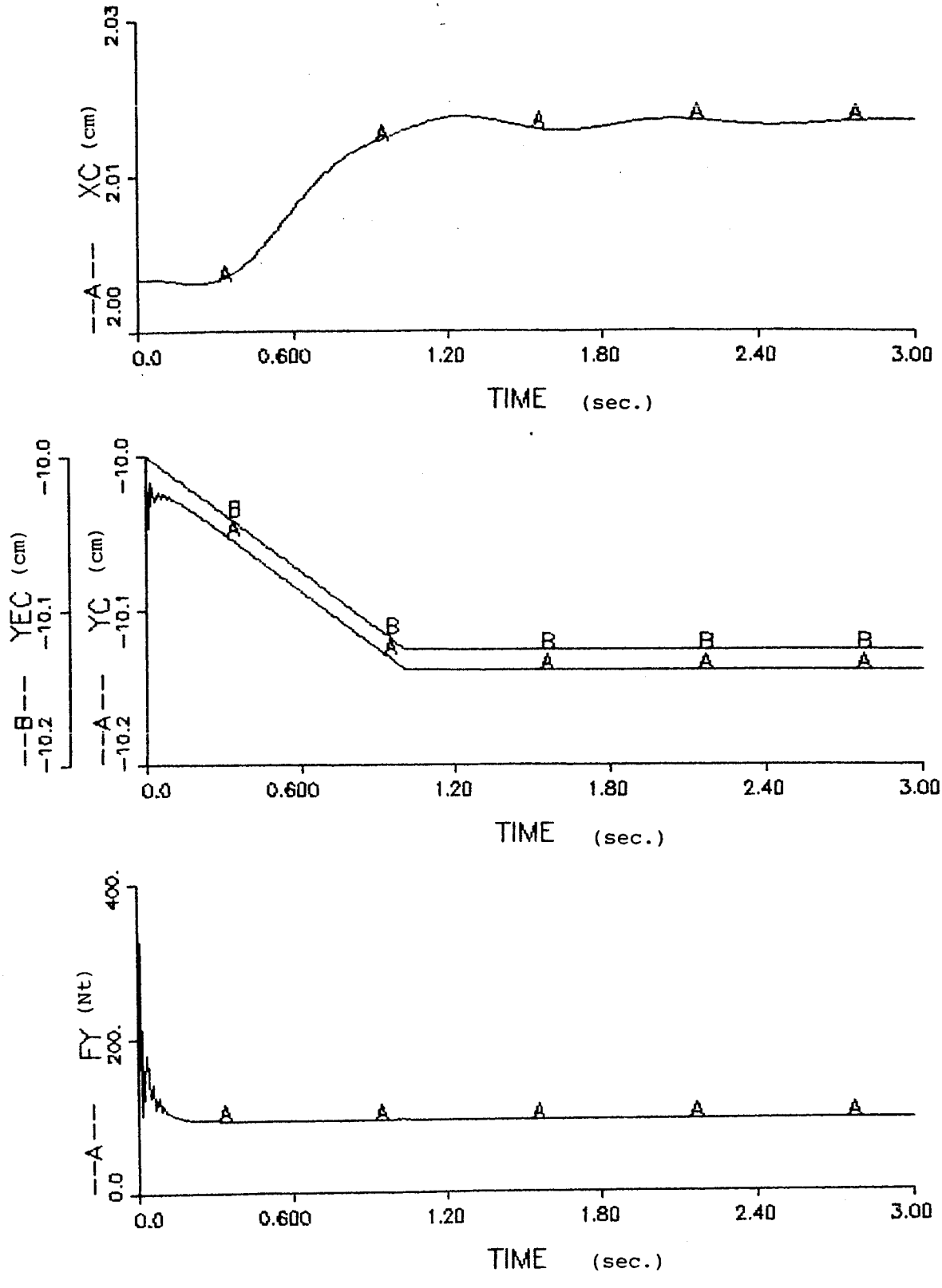

Fig. 13: Responses for Control of Constant Force on a Moving Table (V_{table} = 0.1 cm/sec)

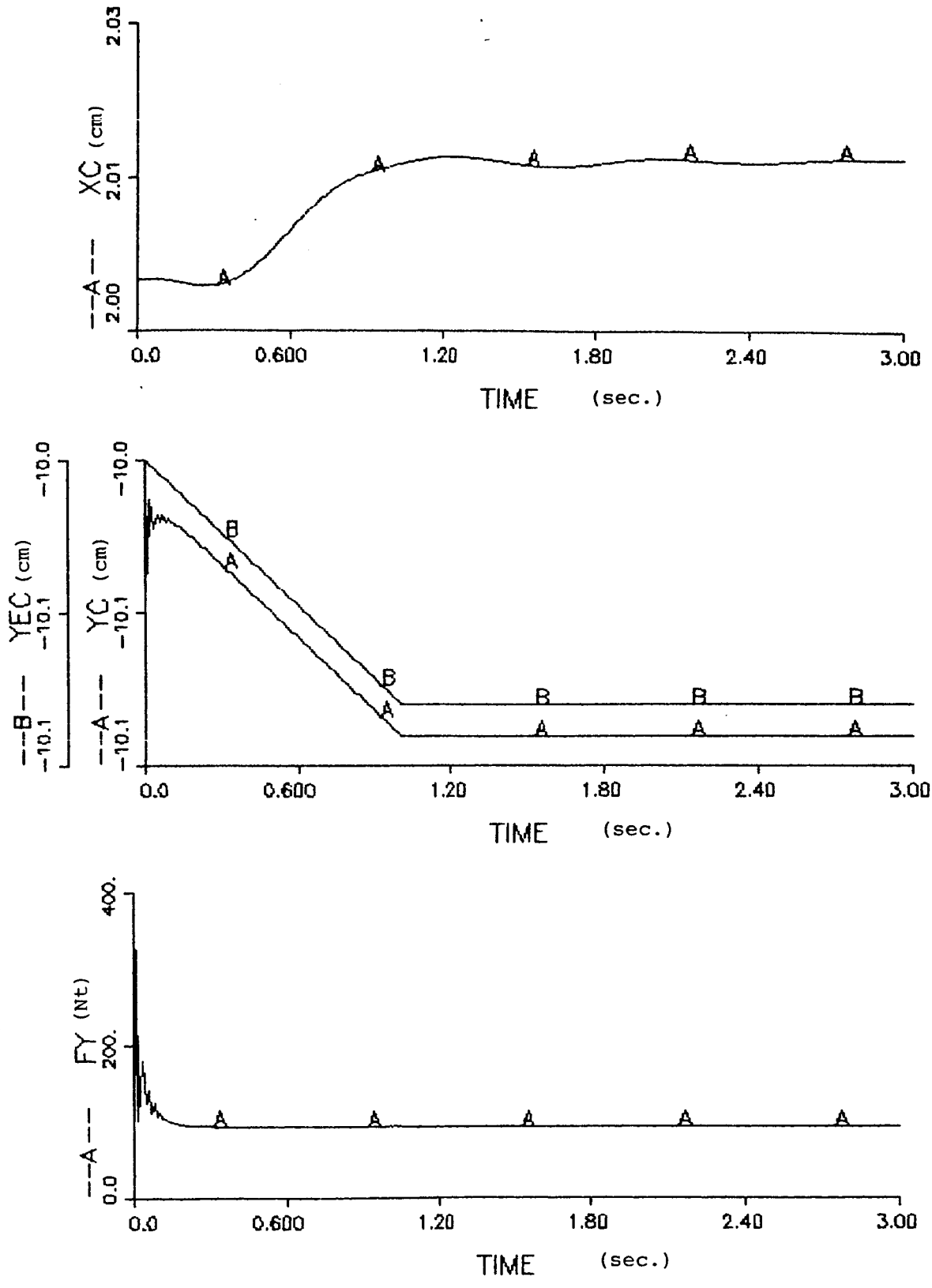

Fig. 14: Responses for Control of Constant Force on a Moving Table (V_{table}= 0.08 cm/sec)